Ultracold neutrons

ideal gas with temperature of milli-Kelvin

move with velocities of few m/s

strong	magnetic	gravitation
Fermi potential V_F	**$V_m = -\mu B$**	**$V_g = m_n gh$**
⇓	⇓	⇓
200 neV	**60 neV T^{-1}**	**100 neV m^{-1}**
	⇓	⇓
$E_n < 200$ neV	**3.3 T field → 200 neV**	**2 m → 200 neV**

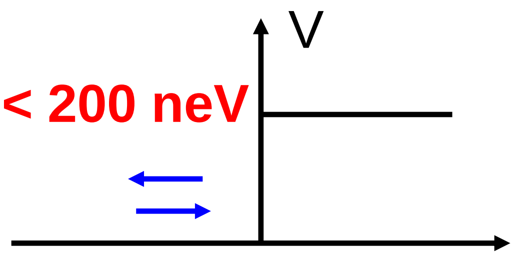

The main paths to many free neutrons

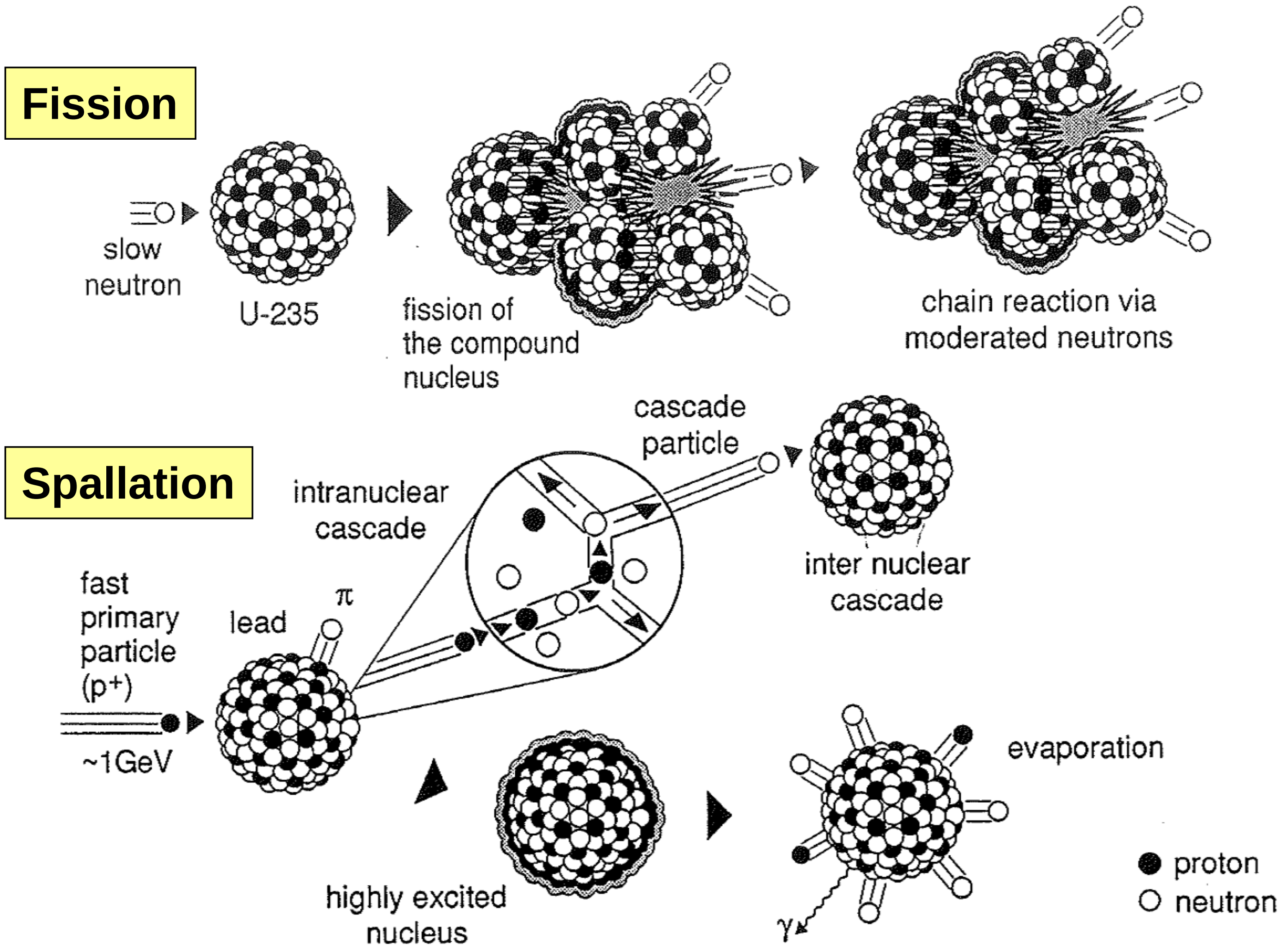

Energy distribution of fission/spallation neutrons

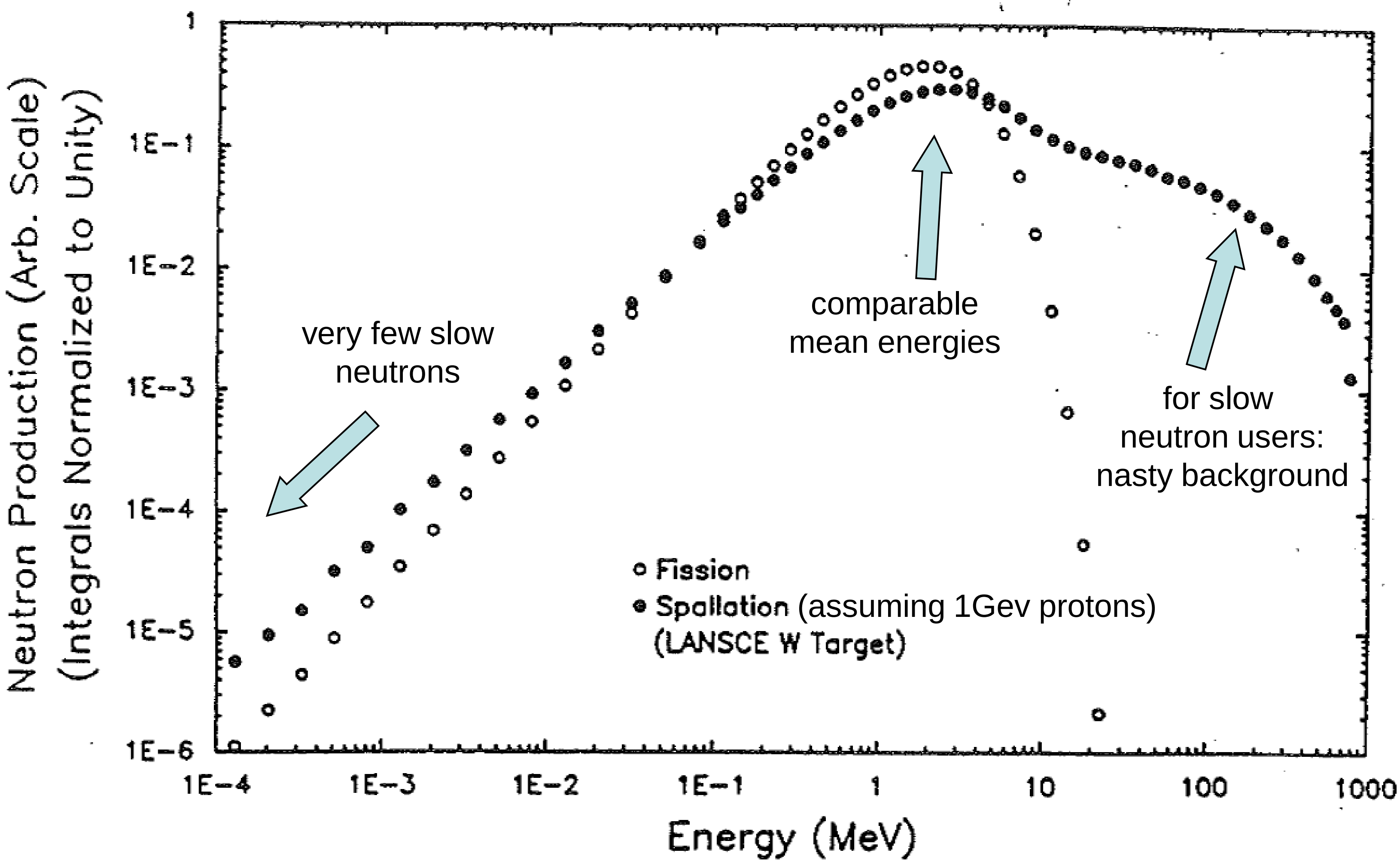

Parameter	Element					
	H	D	Be	C	O	U
A	1	2	9	12	16	238
ξ	1.000	0.725	0.209	0.158	0.120	0.00838
x (2 MeV $\rightarrow$ 25 meV)	18	25	86	114	150	2172

Table 3: Slowing-down parameters of various elements [5]

the shortest possible time. An important quantity to characterize a moderator is its mean logarithmic energy decrement per collision, ξ, which is for all practical purposes given by

$$\xi = lnE_0 - lnE_1 \approx \begin{cases} \dfrac{2}{A+2/3} & \text{for} \quad A \geq 2 \\ 1 & \text{for} \quad A = 1 \end{cases} \tag{3.1}$$

with E_0 and E_1 being the neutron energies before and after the collison and A the atomic number of the moderator atom. So, hydrogen is the most effective moderator in terms of energy transfer per collision.

This allows to calculate immediately the average number of collisions x, to shift the spectrum from one mean energy value to another. For E_0 = 2 MeV and E_f = 25 meV, one has for example:

$$x = \frac{1}{\xi} \cdot ln\frac{E_0}{E_f} = \frac{1}{\xi} \cdot ln(8 \cdot 10^7) = \frac{18.2}{\xi}. \tag{3.2}$$

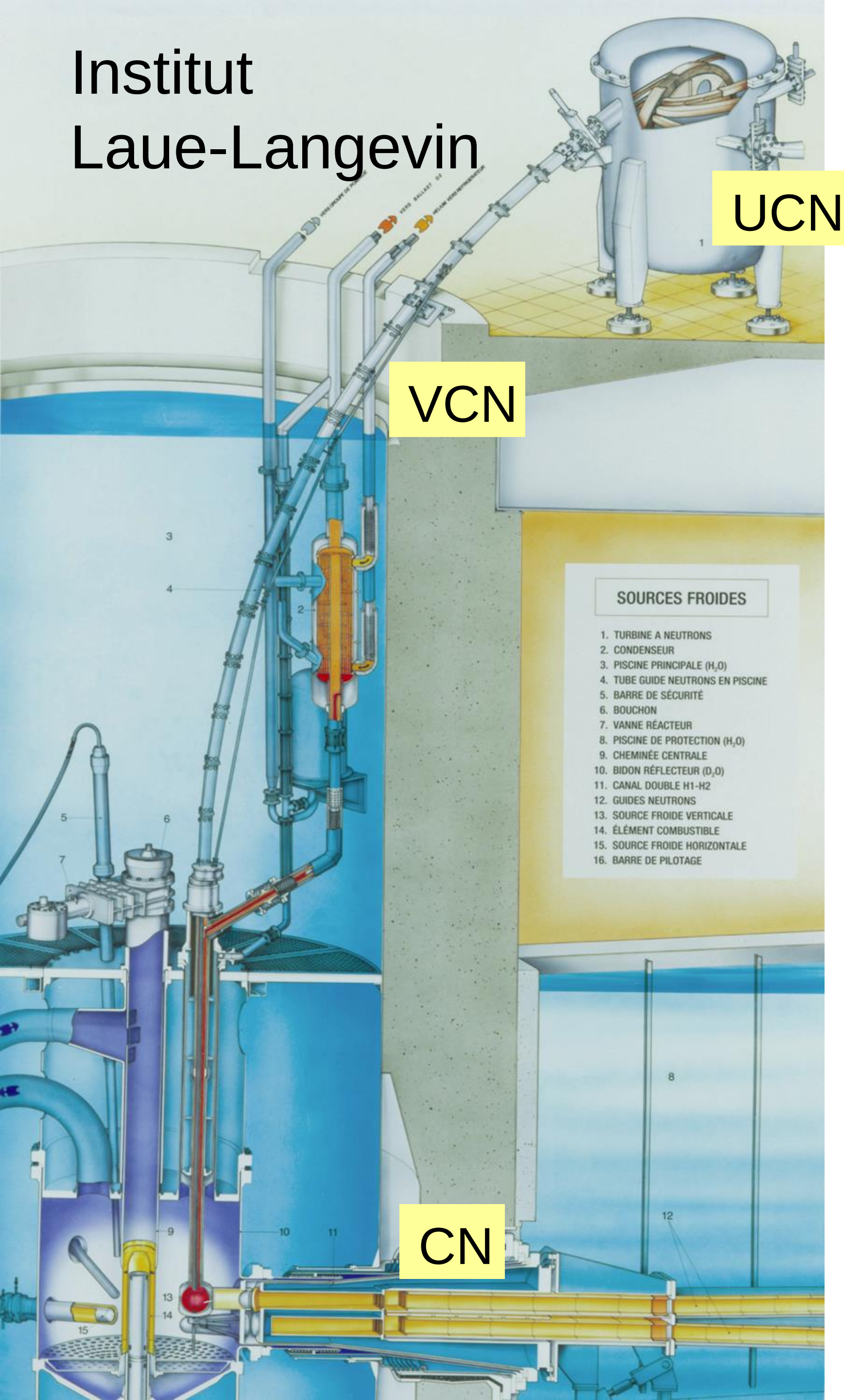

Neutron production: moderation & thermal equilibrium

Maxwell-Boltzmann

$$\rho(v)dv = \frac{2\Phi_0}{\alpha}\frac{v^2}{\alpha^2}exp(-v^2/\alpha^2)\frac{dv}{\alpha}$$

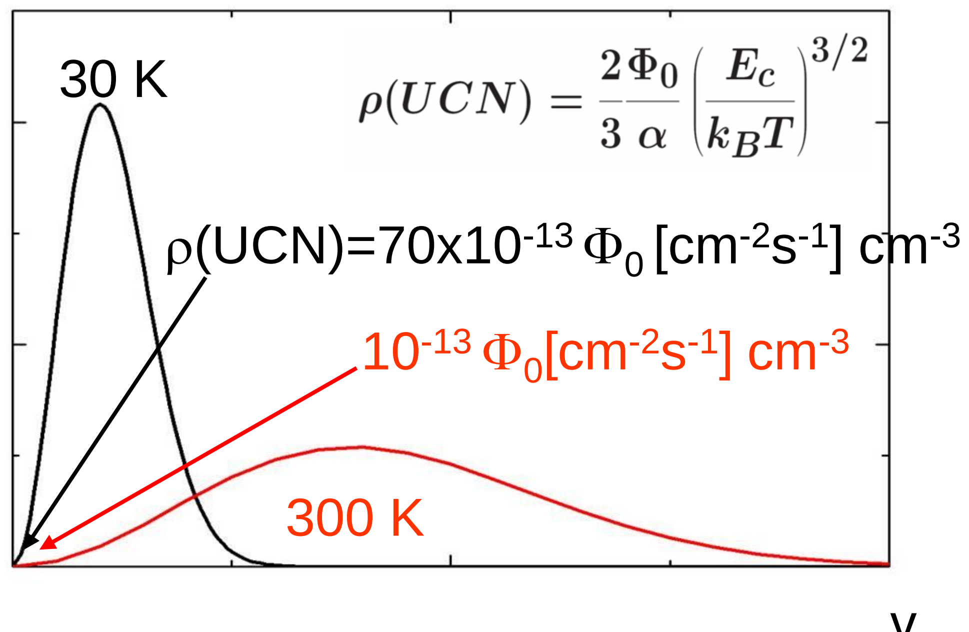

$\alpha=(2k_BT/m)^{1/2}$

Superthermal UCN production

- Golub and Pendlebury, PL62A(1977)337: superfluid He
- Golub and Böning, ZPB51(1983)95
Yu, Malik, Golub, ZPB62(1986)137 } solid D_2

$$\boxed{\rho_{UCN} = \Phi_{CN}\, \Sigma\, \tau_{UCN}}$$

He: small Σ, long τ
D_2: large Σ, small τ

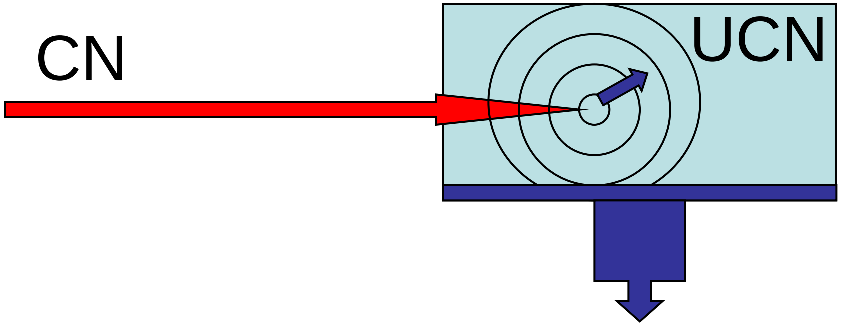

Detailed balance:
upscattering cross section =
exp($-\Delta E/kT$) x downscattering

Cooling machine = phonon pump

CN energy dependent UCN production

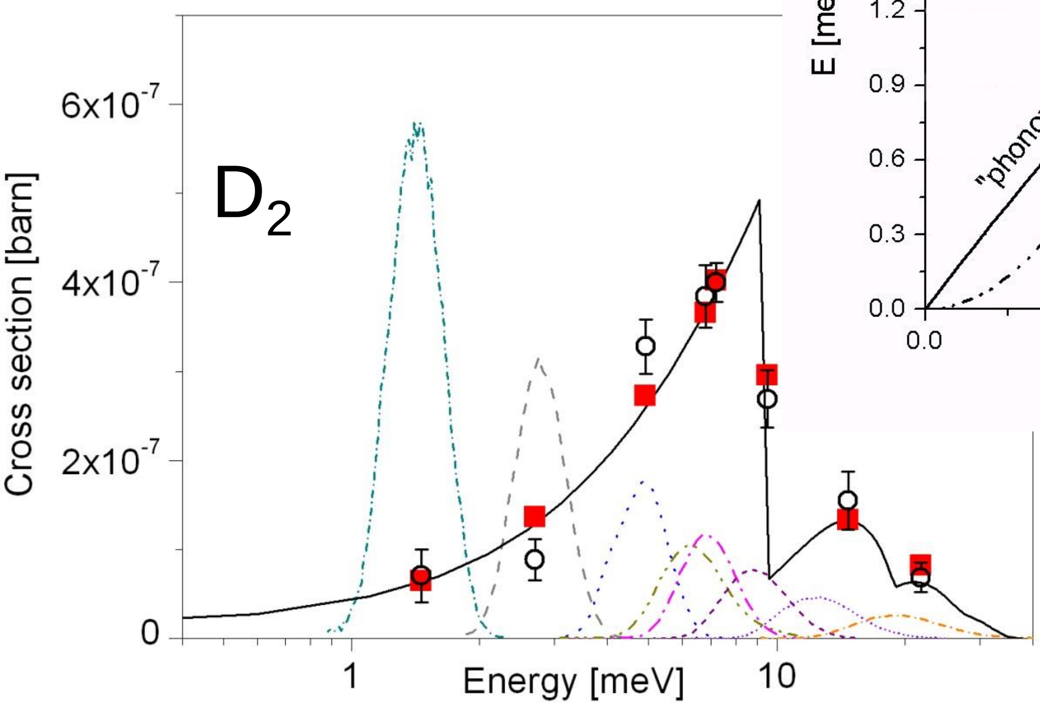

F. Atchison et al., PRL99(2007)262502

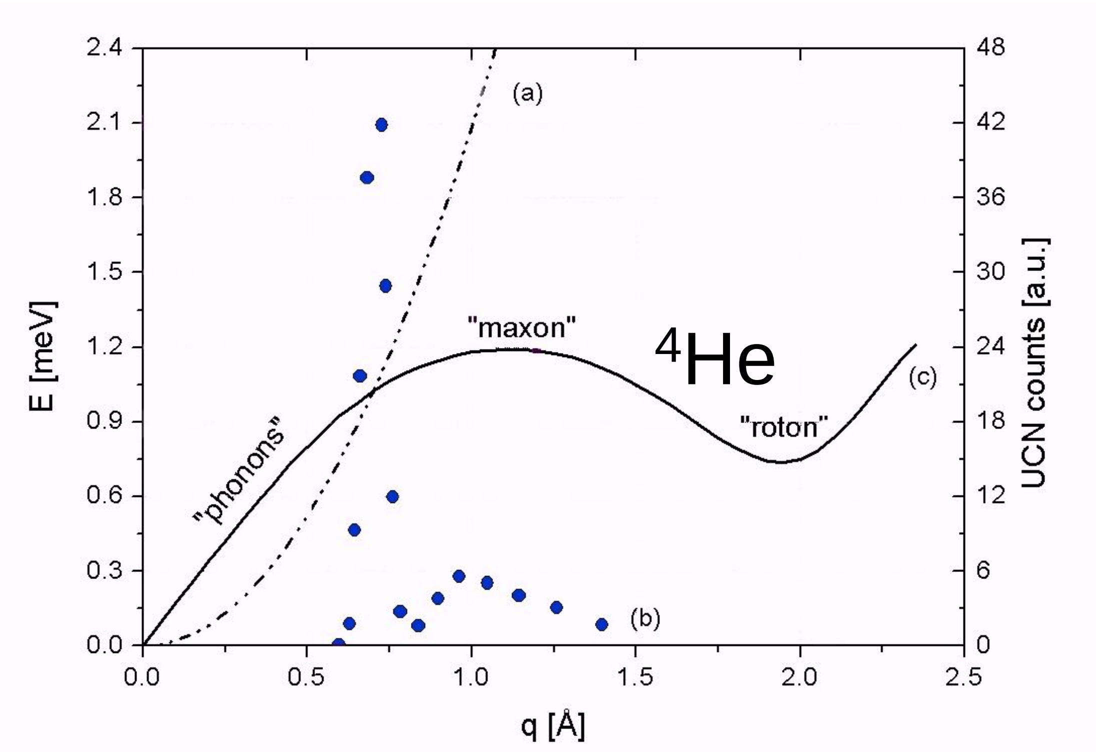

C.A. Baker et al., PLA308(2003)67

for crude estimates …

$$\rho_{UCN} = \Phi_{CN}\, R\, \tau_{UCN}$$

	R [cm^{-1}]	τ_{UCN} [s]
D_2	10^{-8}	0.03…0.1
He	1..3 x 10^{-9}	10…1000

… inside He-II one can in principle produce about 2 orders of magnitude higher UCN density from the same cold neutron flux than inside solid D_2, but ...

Y.N. Pokotilovski / Nucl. Instr. and Meth.

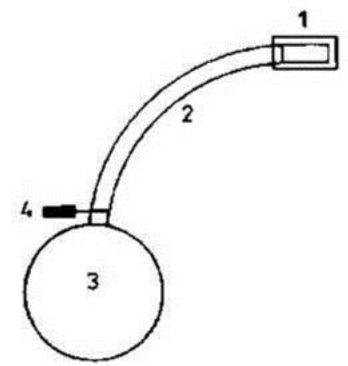

Fig. 1. The principal scheme of the method: 1) The cooled moderator-converter of UCN. 2) The curved mirror neutron guide. 3) The camera for storage of UCN. 4) The shutter for UCN.

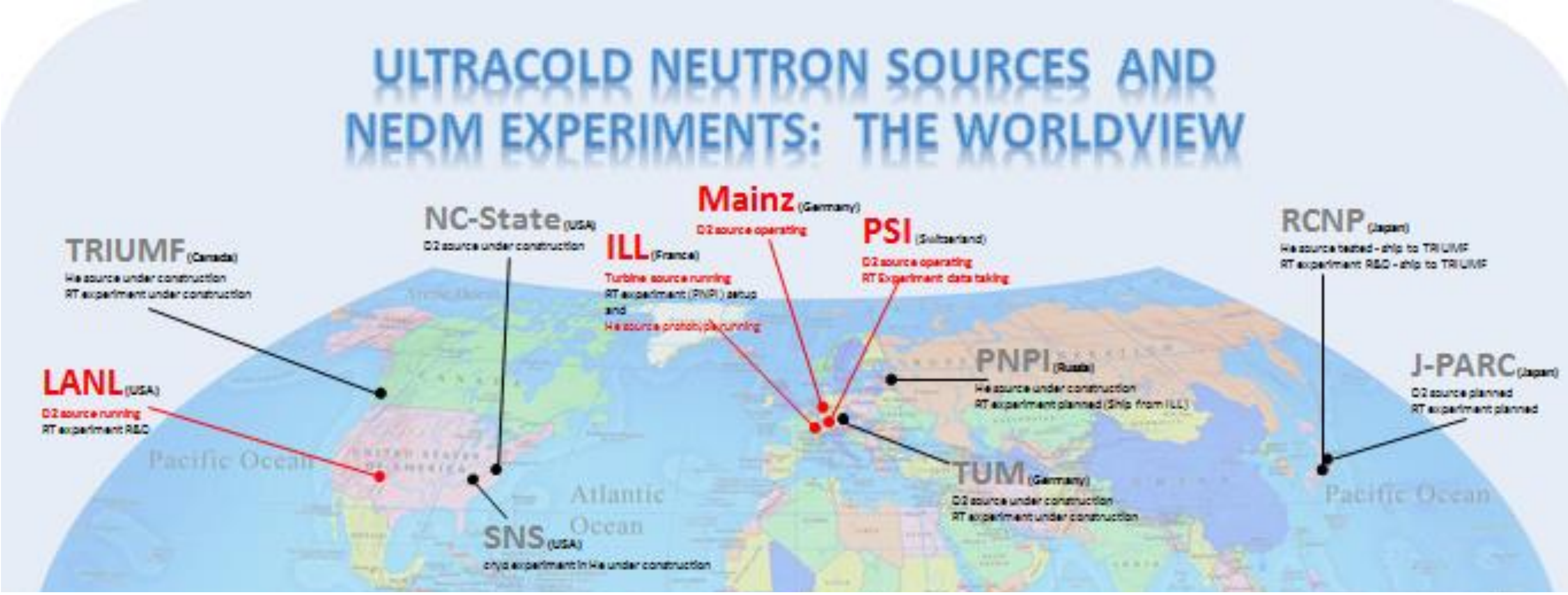

TABLE 2. UCN sources and source projects worldwide.

	UCN source location	Technique n-source, moderator, converter	Reference	Comment
1	ILL Grenoble, France	fission, D_2O, liquid D_2, turbine	[17]	operational
2	LANL, USA	spallation, C-Be-PE, solid D_2	[18]	operational
3	PSI, Switzerland	spallation, D_2O, solid D_2	[19]	operational
4	TRIGA Mainz, Germany	fission, C-H_2O, solid D_2	[20]	operational
5	PULSTAR, NCSU, USA	fission, D_2O, solid CH_4, solid D_2	[21]	design/construction
6	FRM-2, Germany	fission, D_2O, solid D_2	[22]	design/construction
7	ILL Grenoble, France	fission, CN beam, SF-He	[23, 24]	operational
8	RCNP Osaka, Japan	spallation, C, solid D_2O, SF-He	[25]	operational
9	TRIUMF, Canada	spallation, D_2O, liquid D_2, SF-He	[40]	design/construction
10	PNPI Gatchina, Russia	fission, C, liquid D_2, SF-He	[27, 28]	design/construction
11	ESS Lund, Sweden	spallation	[32, 33]	under discussion

Bottle of wine question:

- To a slow neutron, all nuclei are attractive potential wells from 10 to 60 MeV deep and a few fm in diameter. Nevertheless, most elements, when made into mirrors, reflect (i.e., repel) slow neutrons. Why??

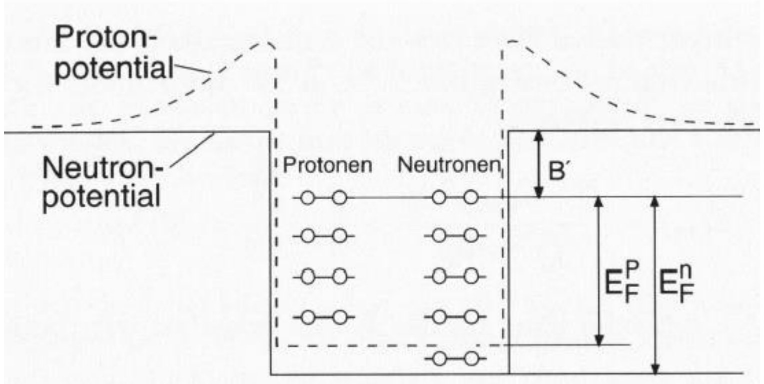

  - Answers that reach me by 8pm today in form of 1 page handwritten short explanations take part in the competition.
  - The winner will get the bottle of sparkling wine which I brought ('Engelhof' 2012 Rivaner Brut)

Scattering of a slow neutron

Approximate nuclear potential as spherical square-well

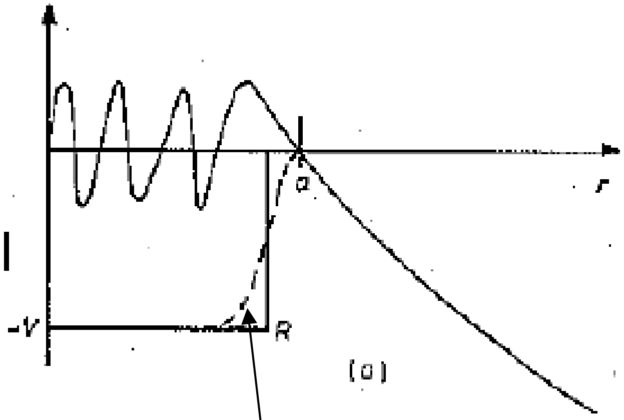

here, we don't have to care for the specific form of the potential

2.2 SCATTERING FROM A SINGLE NUCLEUS

2.2.1 The scattering length

Approximate nuclear potential as spherical square-well

For slow neutrons with de Broglie wavelength λ satisfying

$$kR = \frac{2\pi R}{\lambda} \ll 1$$

R is the nuclear radius. The neutron wavelength λ is much larger than R

the wavefunction for $r > R$, i.e. the region where $V(r) = 0$, has the form of a spherical wave $\sim e^{ikr}/r$. For $r < R$, the wavefunction $u = r\psi$ has the form (for the spherical square-well potential)

$$u \sim A \sin Kr \qquad K = \sqrt{\frac{2m(E + V_0)}{\hbar^2}} \tag{2.7}$$

satisfying the boundary condition $u = 0$ at $r = 0$.

In general $KR \gg 1$ so that u makes several oscillations inside the potential well before joining the external wavefunction at $r = R$. Thus we can write for the total wavefunction outside the well (incident plane wave $e^{i\boldsymbol{k}\cdot\boldsymbol{r}}$ plus scattered wave)

$$\psi = e^{i\boldsymbol{k}\cdot\boldsymbol{r}} + f(\theta)\frac{e^{ikr}}{r}$$

where $f(\theta)$ is determined by the boundary conditions at $r = R$.

With condition (2.6) the scattering is predominantly s wave (

Already for angular momentum 1, the neutron must pass the nucleus at a distance λ out of range for the strong force

$$f(\theta) = \text{constant} = -a \tag{2.10}$$

because any angular dependence of $f(\theta)$ would imply a non-zero angular momentum. Thus for $R < r < 1/k$ we can write (2.8) as

$$\psi \approx 1 - a/r = (r - a)/r \tag{2.11}$$

so that u has the form of a straight line (figure 2.1).

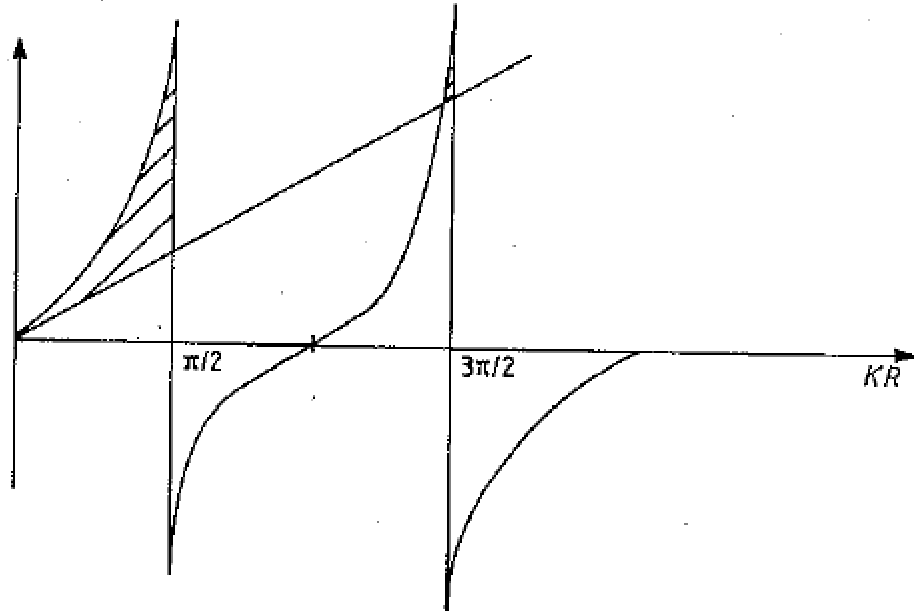

Figure 2.2 Functions relevant to equation (2.12): $\tan KR$ and KR. Shaded regions indicate negative scattering length a.

By applying the boundary condition that u'/u is continuous at $r = R$ we obtain from (2.7) and (2.11)

$$a = R - \frac{\tan KR}{K} = R\left(1 - \frac{\tan KR}{KR}\right). \qquad (2.12)$$

In figure 2.2 we plot $\tan KR$ and KR separately as functions of KR and we see that the shaded regions, where $\tan KR > KR$ are the only places where a can be negative.

Thus except for the first quadrant ($KR < \pi/2$), the regions where $a < 0$ are very small. For all nuclei except hydrogen it turns out that $KR > 3$ so we expect negative scattering lengths to be rare. This is found to be the case in practice as there are only

Sign of the scattering length

repulsive

attractive

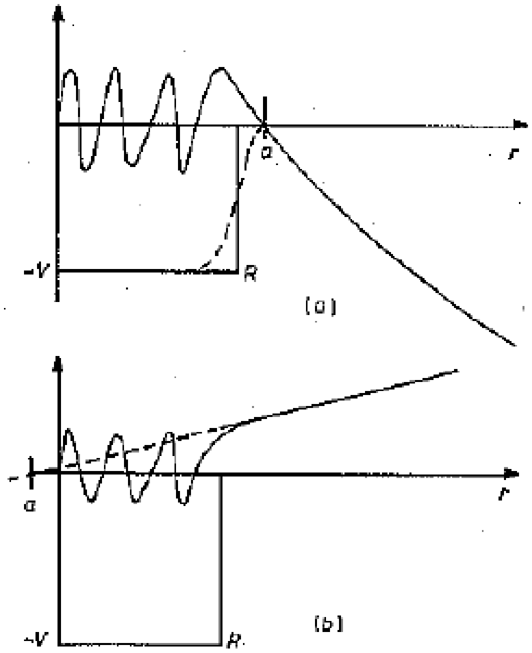

The exact R of a given nucleus and the potential depth determine the boundary condition

Figure 2.1 (*a*) The spherical square-well approximation to the neutron–nucleus interaction potential and the more accurate Fermi form (broken curve) $V_F = V_0/(1 + e^{(r-R)/w})$. The wavefunction for a slow neutron ($\lambda \gg R$) moving in such a potential (equations (2.7) and (2.11)) is shown for the case of positive scattering length, a. (*b*) The wavefunction for the rare case when the strength V and size R of the potential result in a negative a.

Applying the random potential model

NEUTRON SCATTERING AND EXTRA-SHORT-RANGE ... PHYSICAL REVIEW D **77,** 034020 (2008)

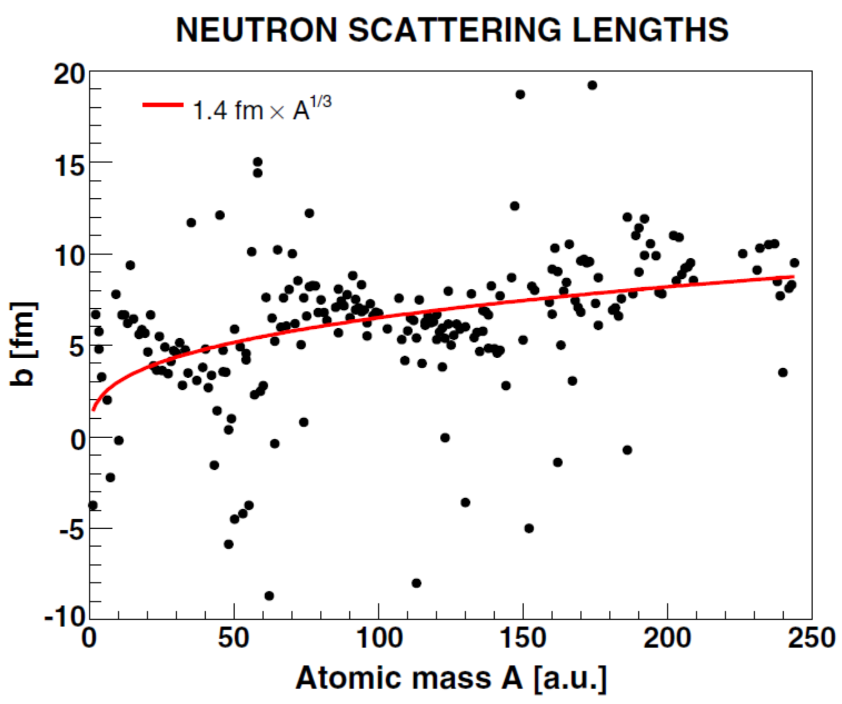

FIG. 1 (color online). Measured scattering lengths as a function of nucleus atomic number.

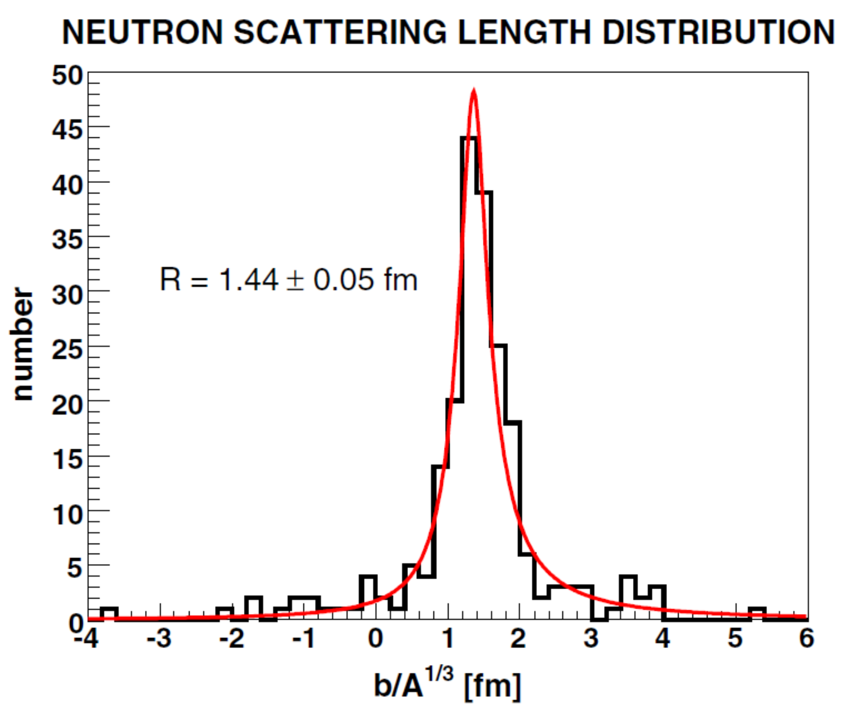

FIG. 2 (color online). This histogram shows the distribution of measured scattering lengths normalized to the radius of the nuclei. The curve corresponds to the random potential model.

$\boxed{\text{see Peshkin and Ringo, Am. J. Phys. 39 (1971)}}$ 324

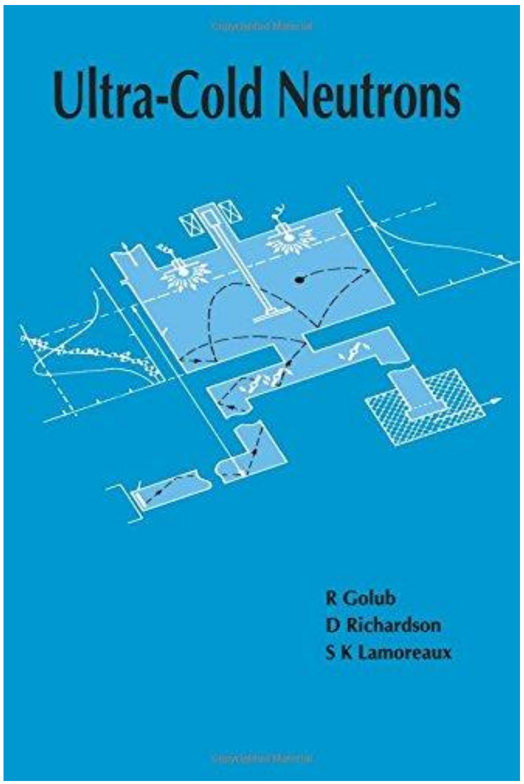

2.4 REFLECTION OF UCN FROM SURFACES

2.4.1 An ideal lossless surface

According to equation (2.46) we can consider the surface of a material with positive scattering length a as constituting a potential step (figure 2.3), of height

$$V = \frac{2\pi\hbar^2}{m} N a \tag{2.47}$$

where N is the number density in the material, which is assumed to be homogeneous. Table 2.1 gives values of V for some common materials.

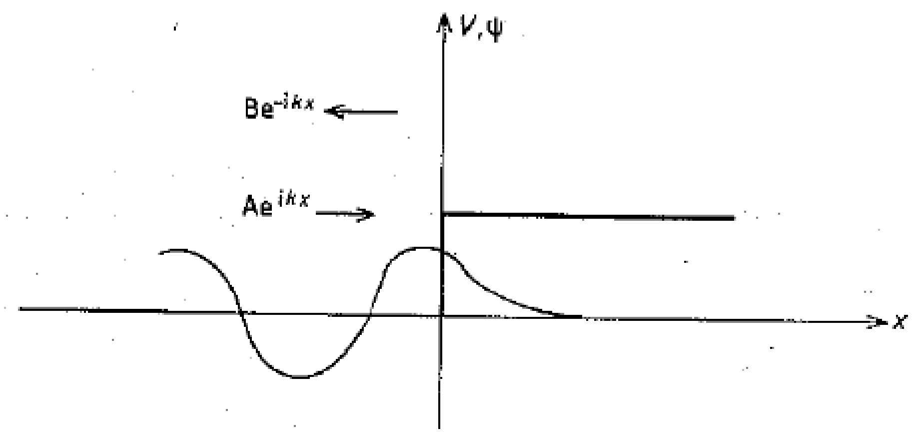

Figure 2.3 Wavefunction of a particle reflected from a material surface represented by a step in potential energy.

Table 2.1 UCN properties of selected materials.

Element	$\rho_{g/cc}$	$N_{form/cc}$ $\times 10^{22}$	$\sum_{form} a_{coh}^{bound}$ $\times 10^{-13}$ cm	V_{neV}	σ_{tot} barns	$f = W/V$ $\times 10^{-5}$
Ni^{58}	8.8	9.0	14.4	335	44	8.6
BeO	3.0	7.25	13.6	261	6.6	1.35
Ni	8.8	9.0	10.6	252	48	12.5
Be	1.83	12.3	7.75	252	1.4[a]	0.5[a]
					0.22[b]	0.08[b]
Cu^{65}	8.5	8.93	11.0	244	28	7.0
Fe	7.9	8.5	9.7	210	30	8.5
C	2.0	10.0	6.6	180	1.4	0.6
Cu	8.5	8.93	7.6	168	43.5	15.5
PTFE (Teflon)	2.2	2.65	17.6	123	—	—
Pb	11.3	3.29	9.6	83	2.0	0.6
Al	2.7	6.02	3.45	54	2.8	2.25
Perspex $(CH_2H_3O)_n$	1.18	1.65	7.88	33.9	—	—
V	6.11	7.1	−0.382	−7.2	50	—
Polyethylene $(CH_2)_n$	0.92	3.9	−0.84	−8.7	—	—
H_2O	1.0	3.34	−1.68	−14.7	—	—
Ti	4.54	5.6	−3.34	−48	58	—

[a] 300 K.
[b] 100 K.

$\rho_{g/cc}$—material density; $N_{form/cc}$—molecular density; $\Sigma_{form}\, a_{coh}^{bound}$—bound co

UCN at the TRIGA Mainz:

beam tube D:

ultra-cold neutrons I

beam tube C:

ultra-cold neutrons II

Courtesy: D. Ries, K. Eberhardt

Pulse Mode Operation

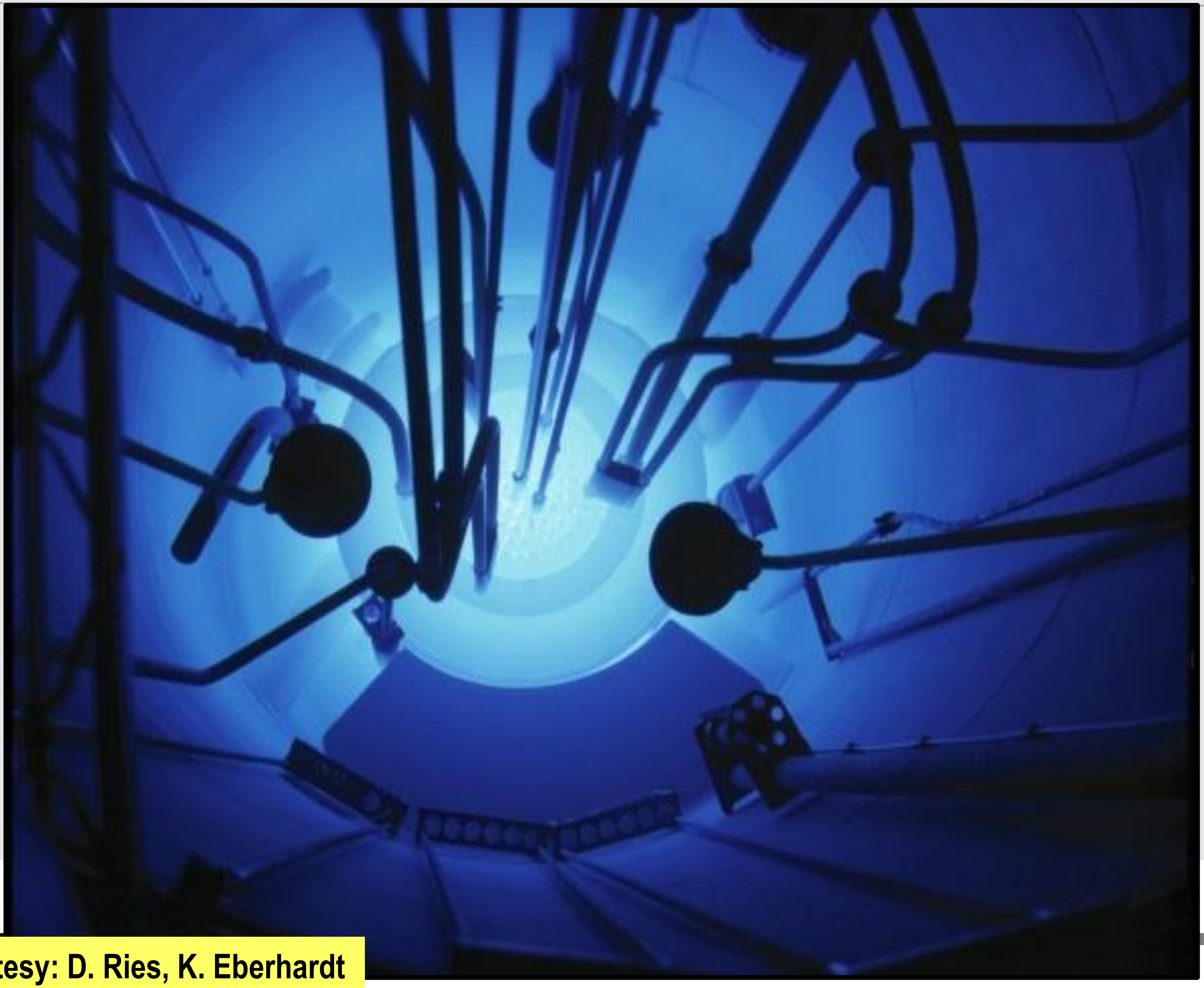

Courtesy: D. Ries, K. Eberhardt

Pulse Mode Operation

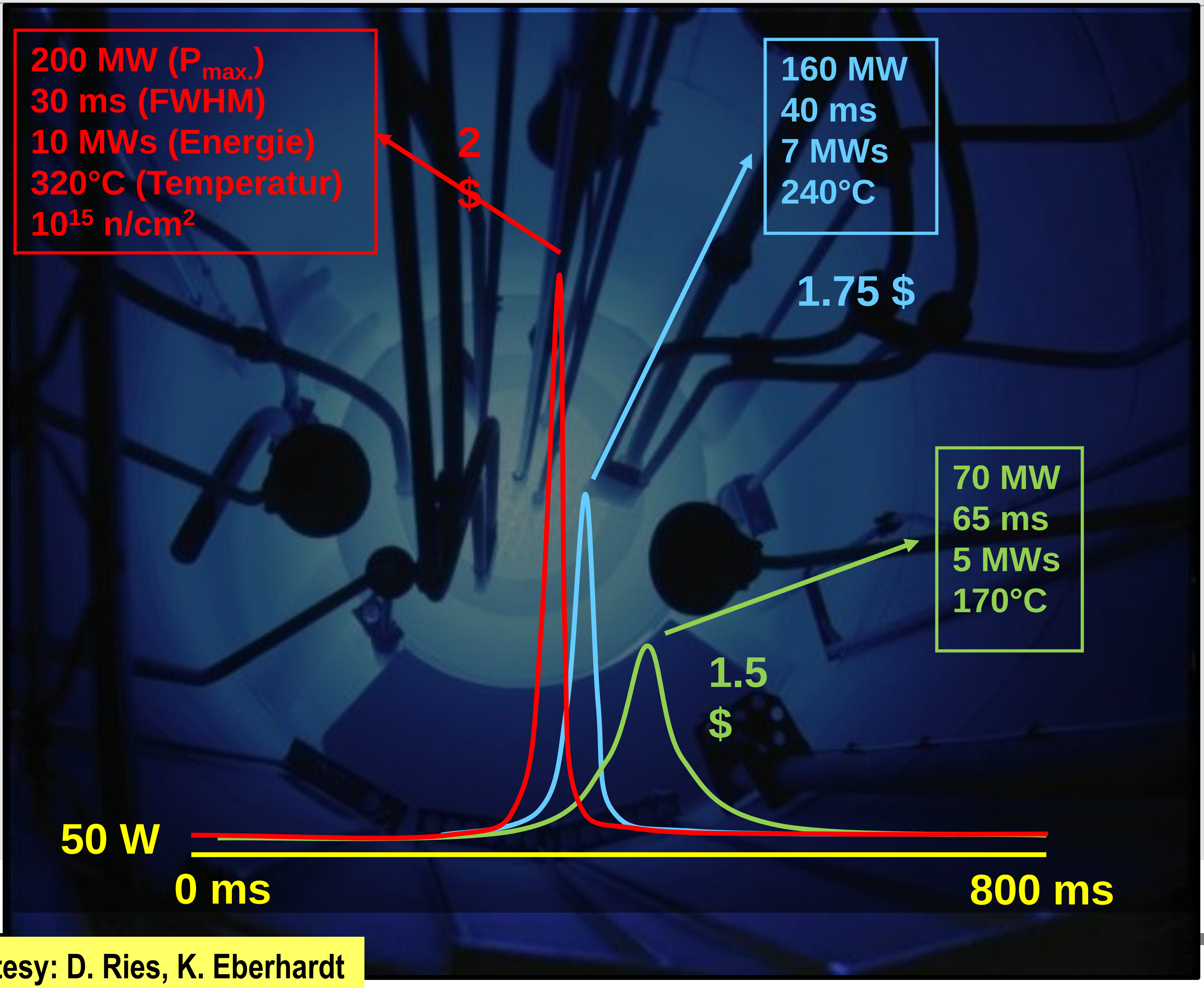

Courtesy: D. Ries, K. Eberhardt

TRIGA UCN Source

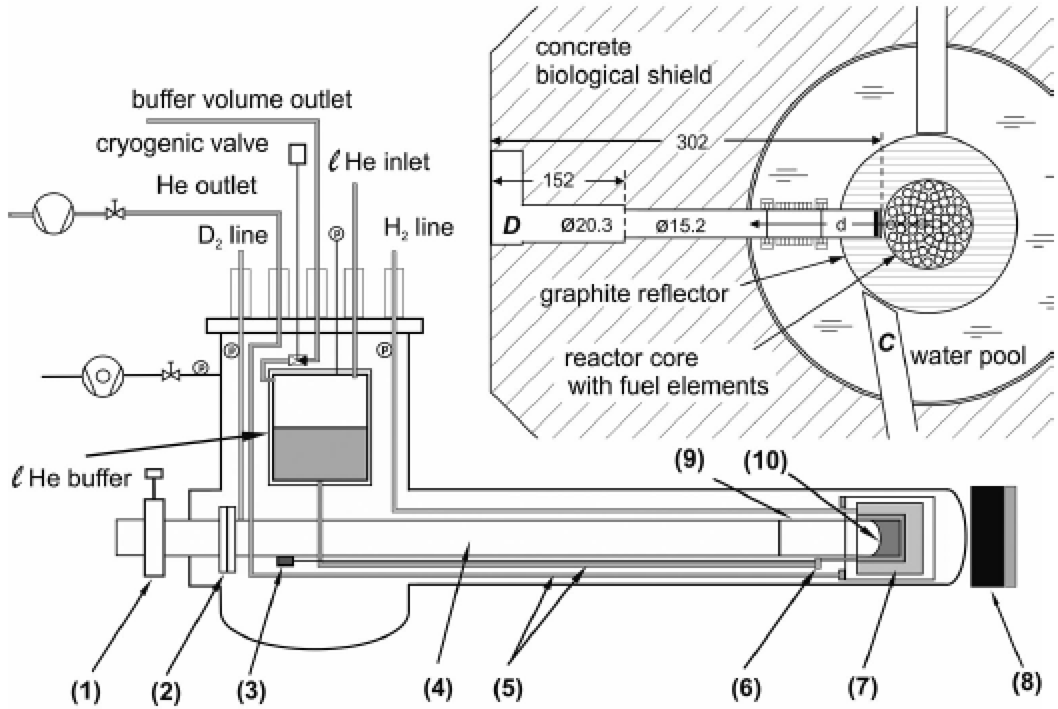

[Karch et al., doi:10.1140/epja/i2014-14078-9, 2014]

- 4) UCN Guide (SS + ^{58}Ni)
- 8) Graphite / Bismuth fast neutron stopper
- 7) Solid H_2 cold moderator
- 10) Solid D_2 UCN converter

Courtesy: D. Ries, K. Eberhardt

Fundamental research UCN – Yields

G. Bison et al.: ***Comparison of ultracold neutron sources for fundamental physics measurements***, *Physical Review C 95; (2017) 045503*

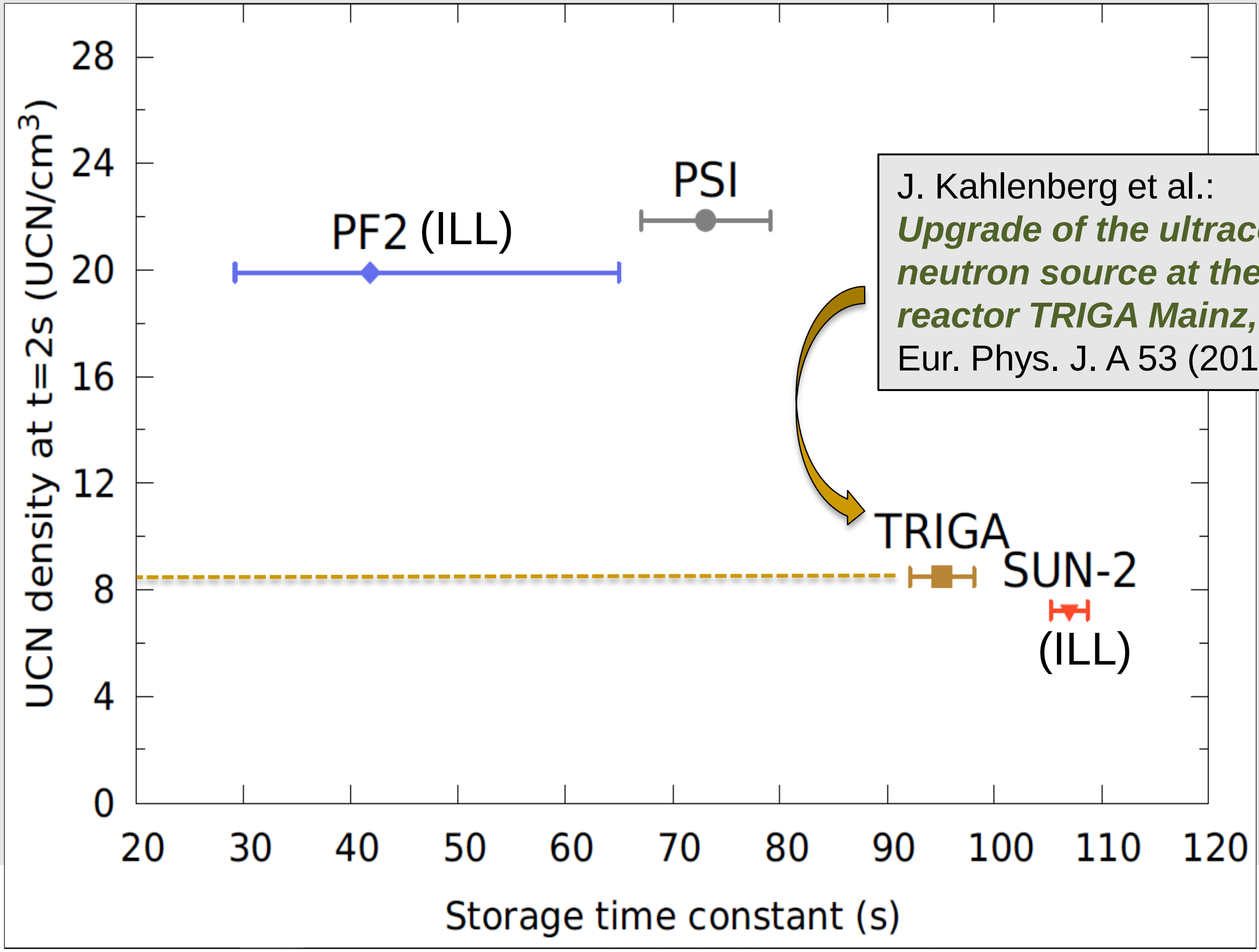

J. Kahlenberg et al.:
Upgrade of the ultracold neutron source at the pulsed reactor TRIGA Mainz,
Eur. Phys. J. A 53 (2017) 226

Courtesy: D. Ries, K. Eberhardt

The intensity frontier at PSI: π, μ, UCN

Precision experiments with **the lightest unstable particles** of their kind

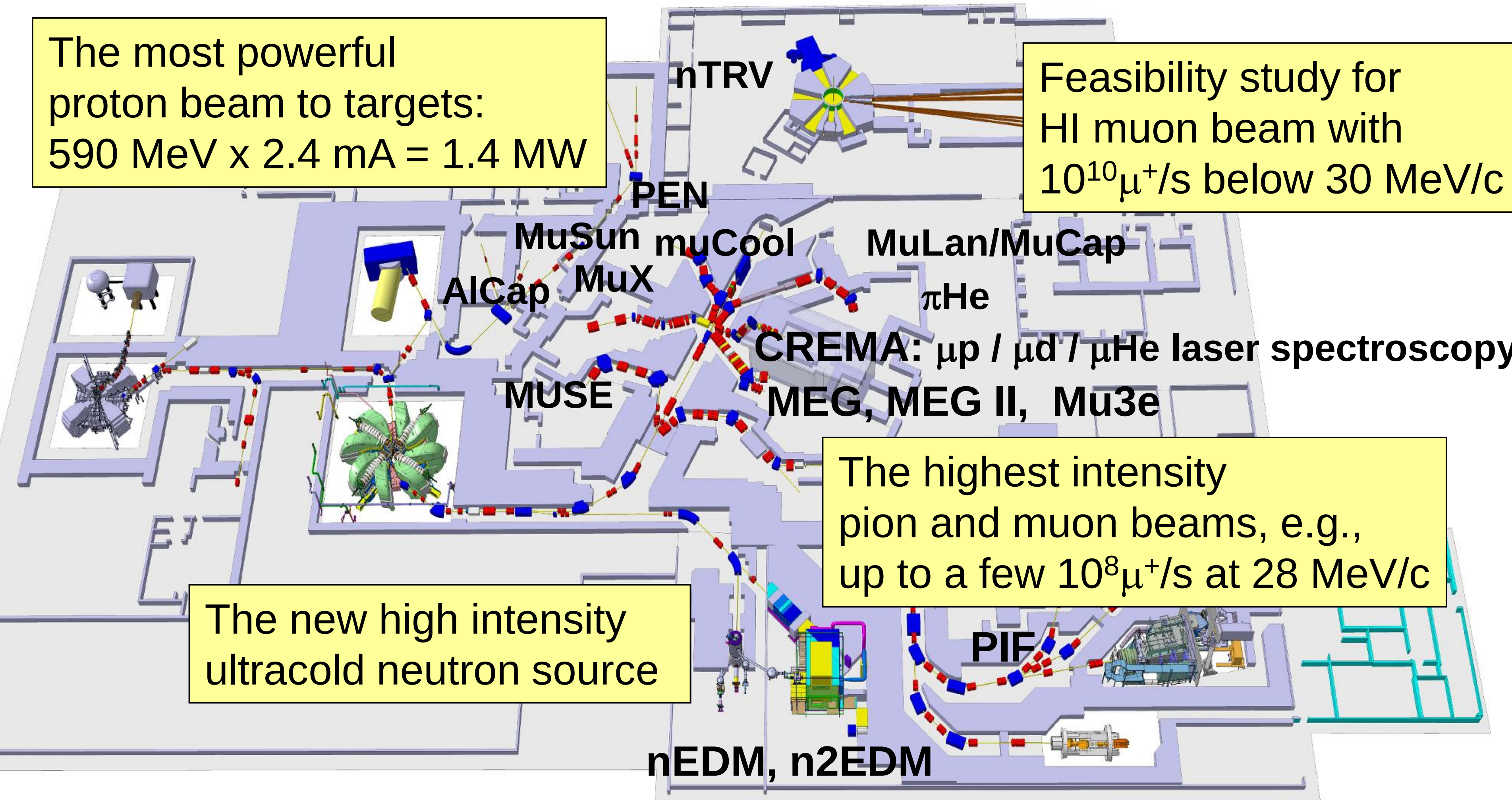

Swiss national laboratory with strong international collaborations

Ultracold Neutron Source & Facility

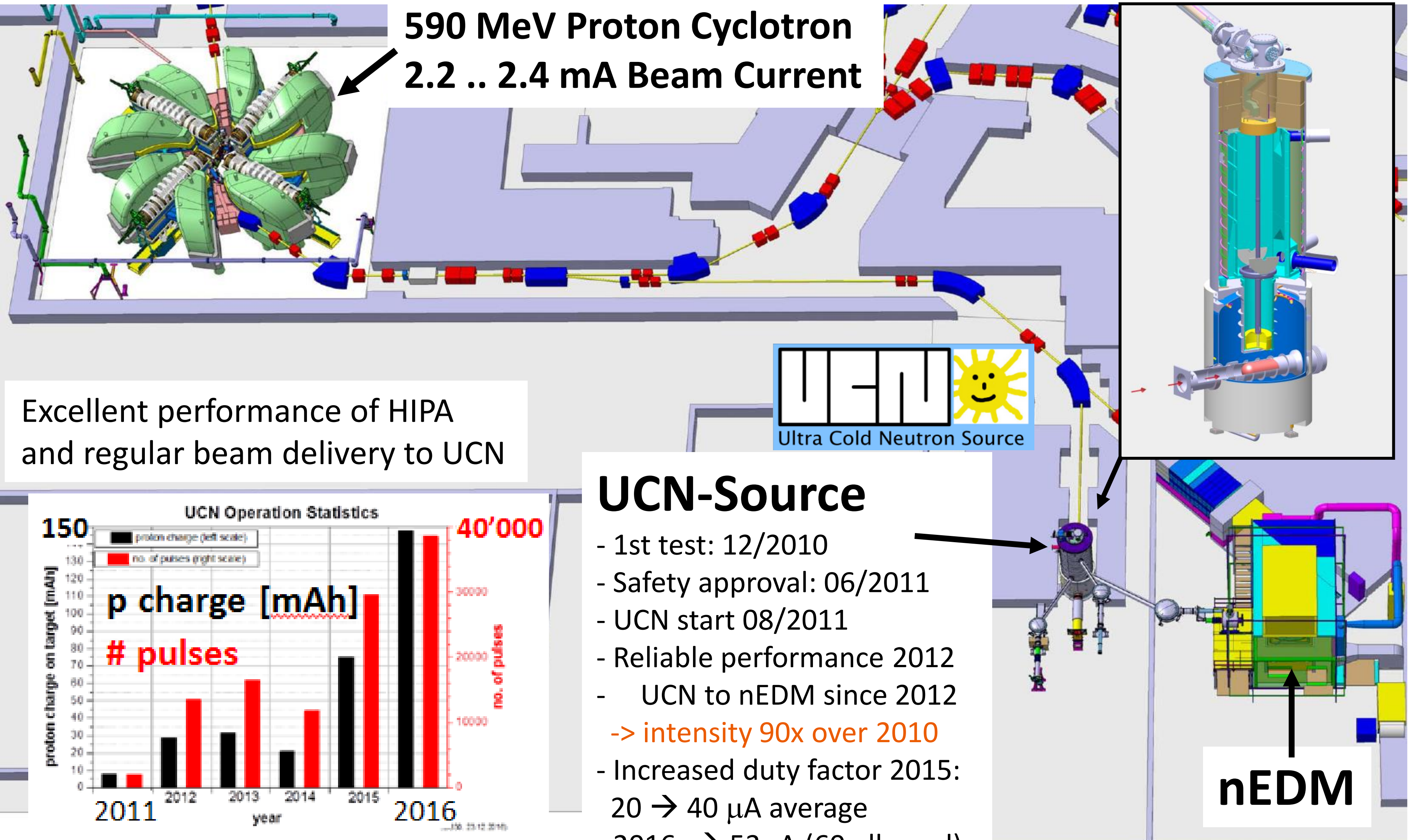

Excellent performance of HIPA and regular beam delivery to UCN

UCN-Source

- 1st test: 12/2010
- Safety approval: 06/2011
- UCN start 08/2011
- Reliable performance 2012
- UCN to nEDM since 2012
  -> intensity 90x over 2010
- Increased duty factor 2015: 20 → 40 μA average
- 2016: → 53μA (60 allowed)

Klaus

The PSI UCN source

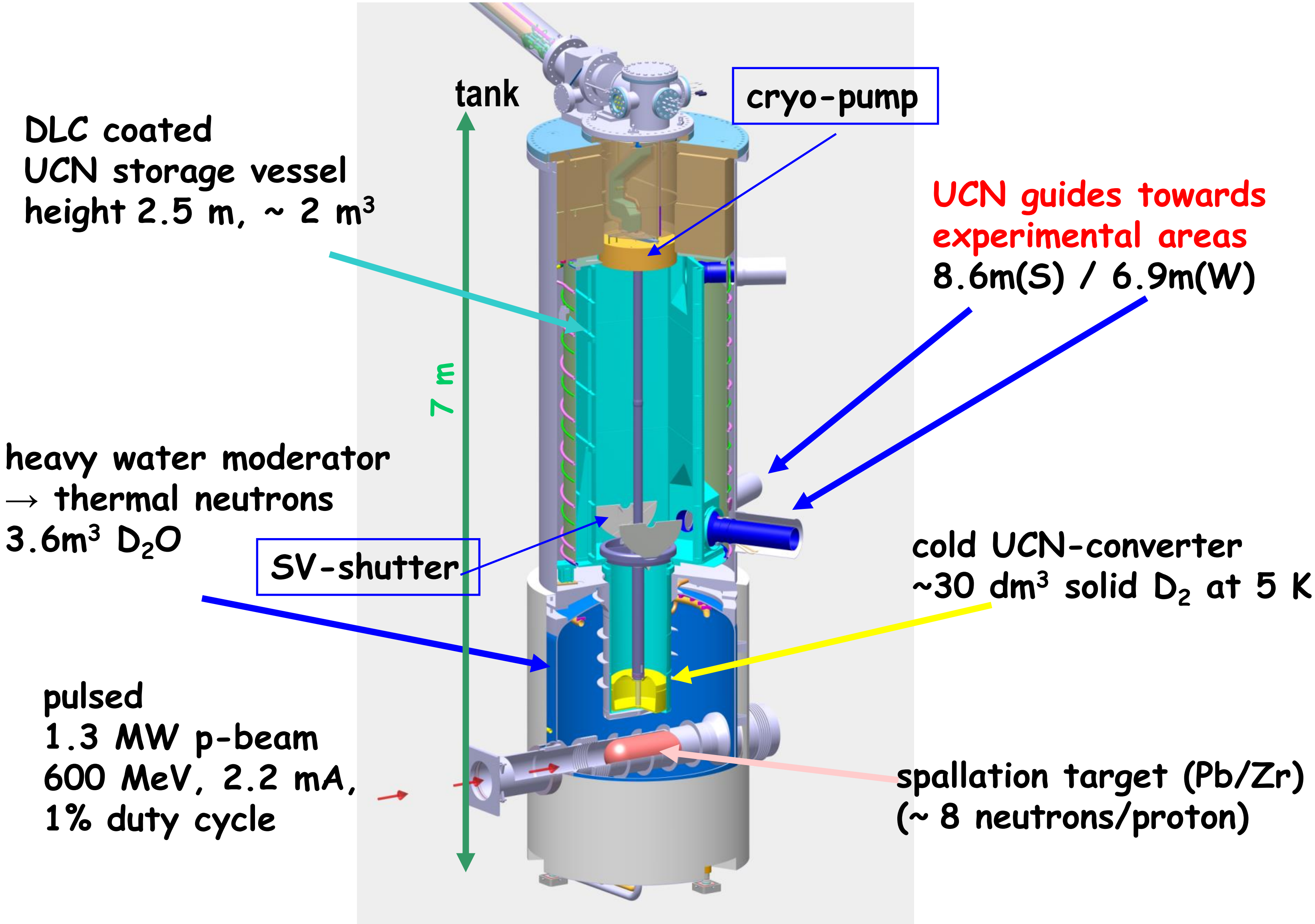

nEDM at PSI 2009 – 17

Coming from ILL:
Sussex-RAL-ILL collaboration
PRL 97 (2006) 131801
Upgraded by nEDM@PSI

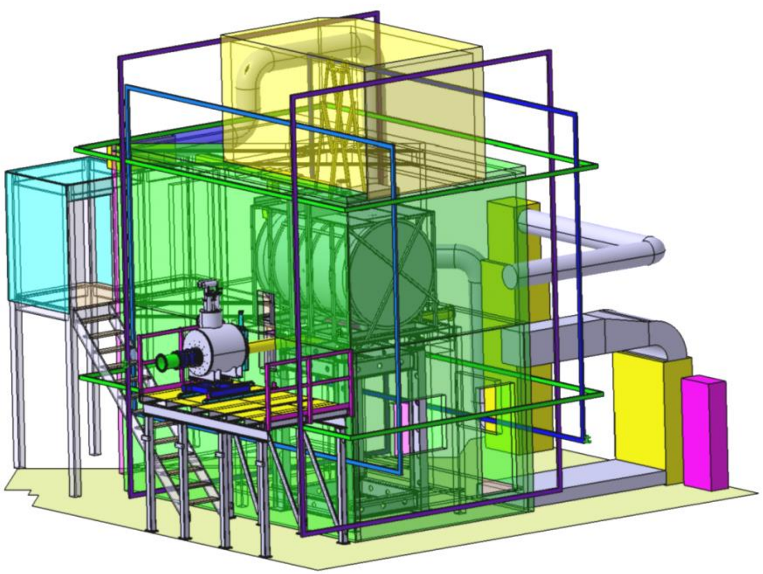

www.psi.ch/nedm/

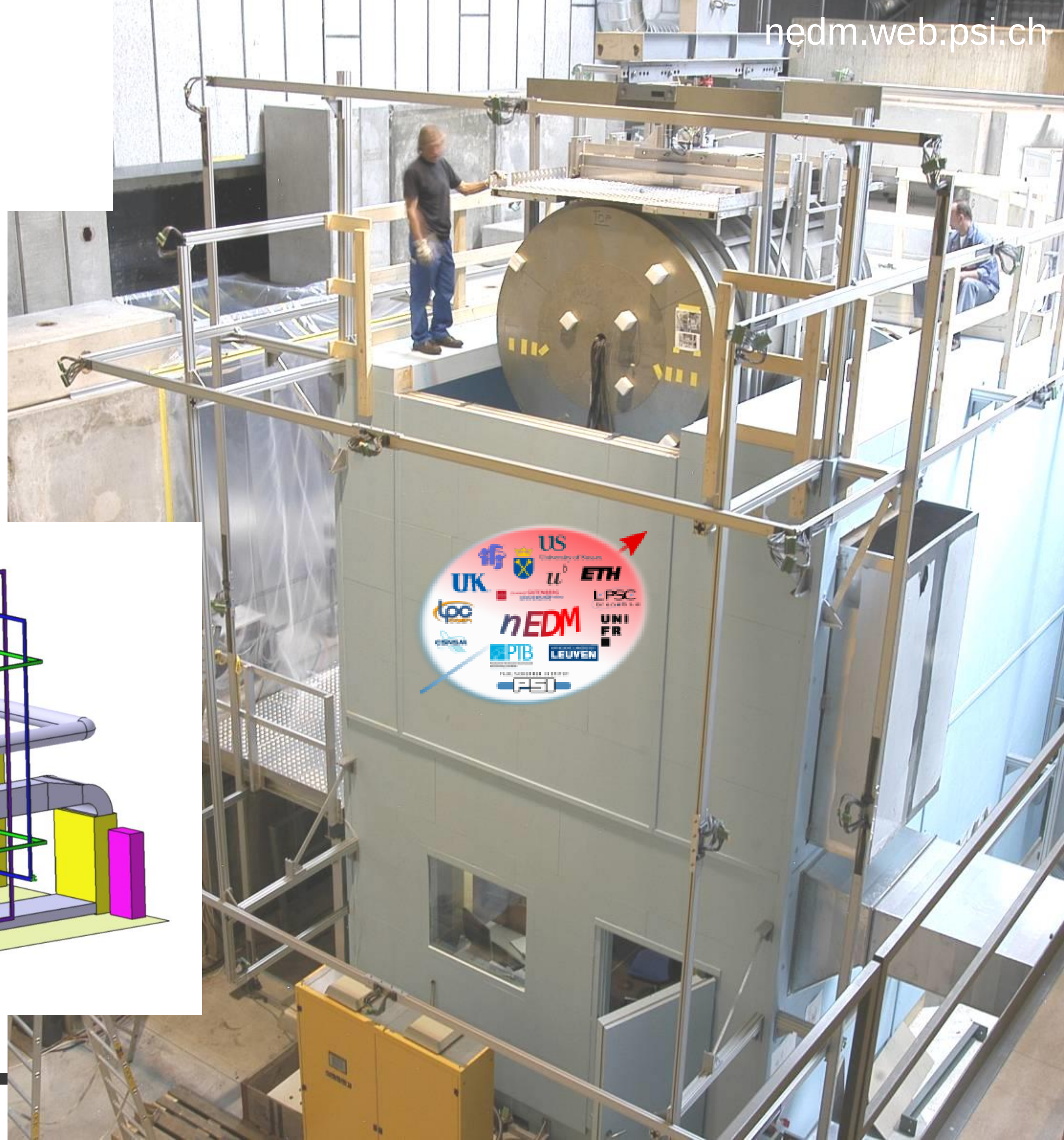

nEDM at PSI

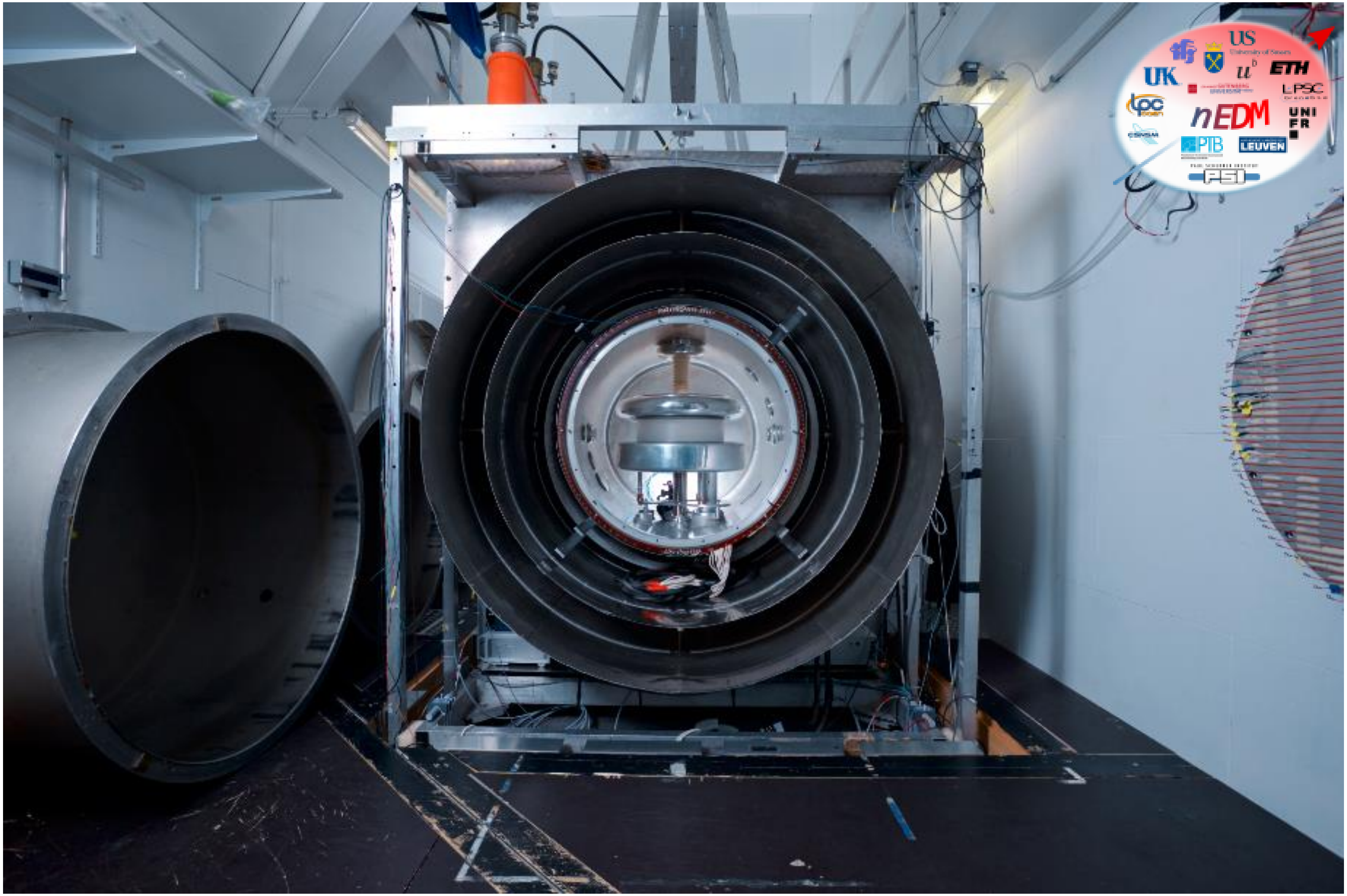

The nEDM spectrometer

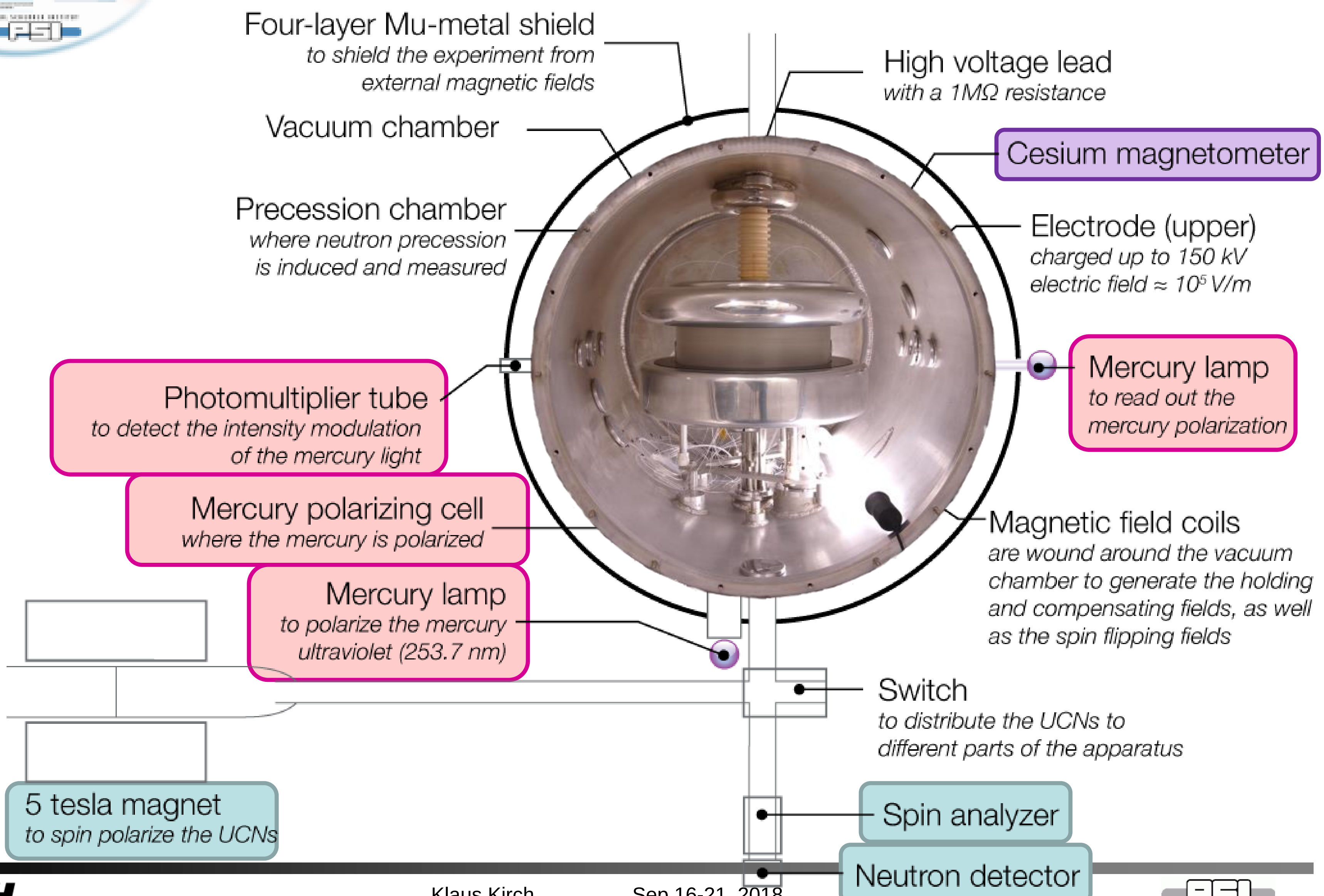

The nEDM spectrometer

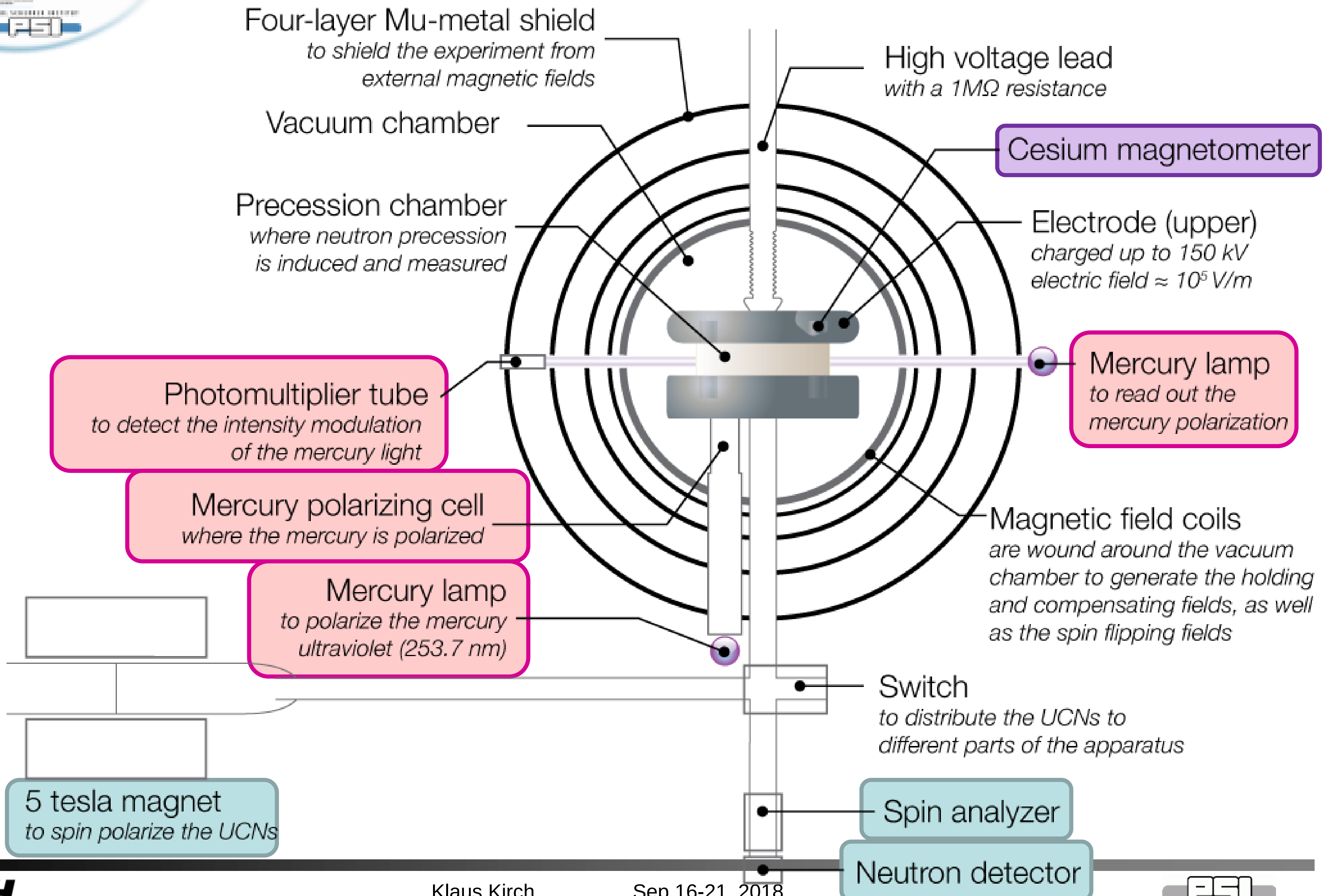

Ramsey's method with UCN

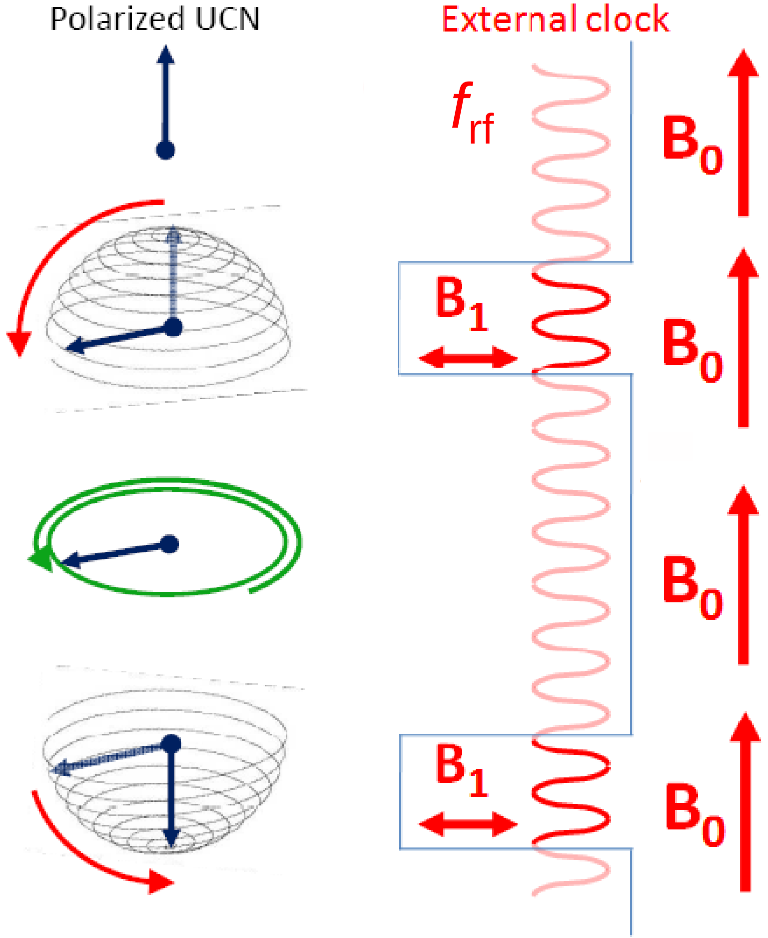

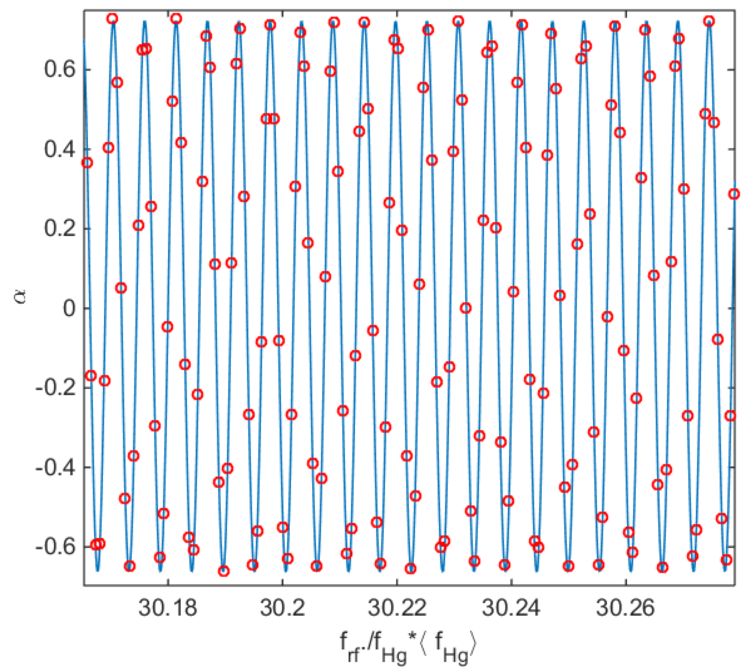

Ramsey's method with UCN

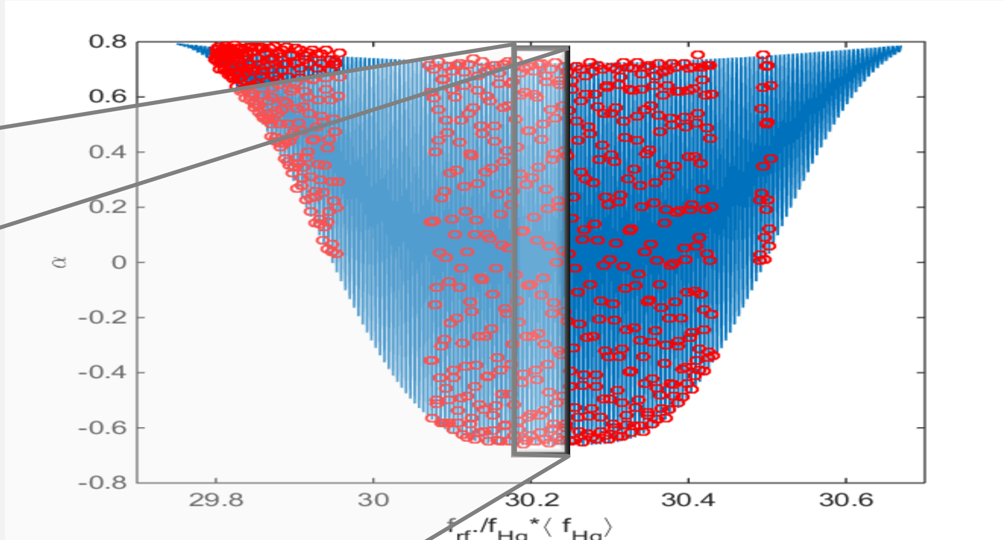

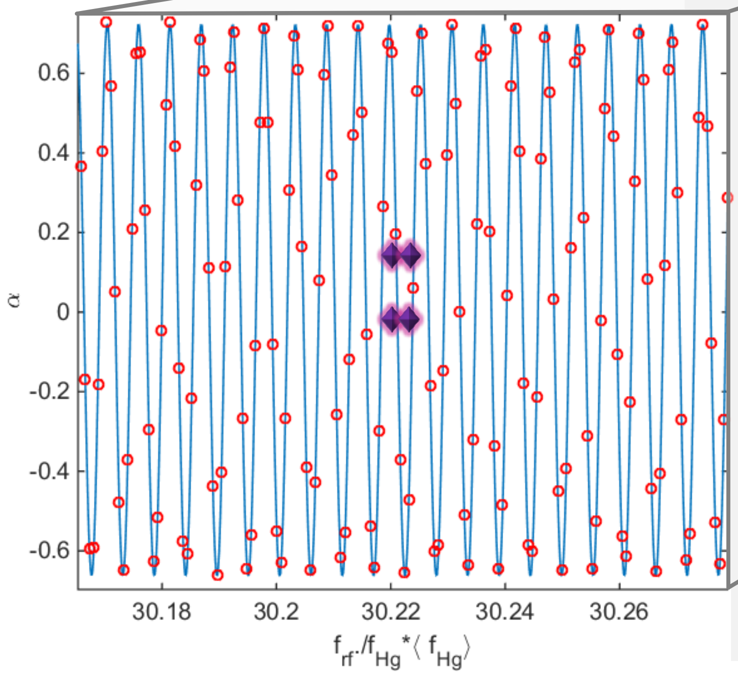

Sensitivity:

$$\sigma(d_n) = \frac{\hbar}{2\alpha T E\sqrt{N}}$$

α	Visibility of resonance
T	Time of free precession
N	Number of neutrons
E	Electric field strength

Frequency ratio R

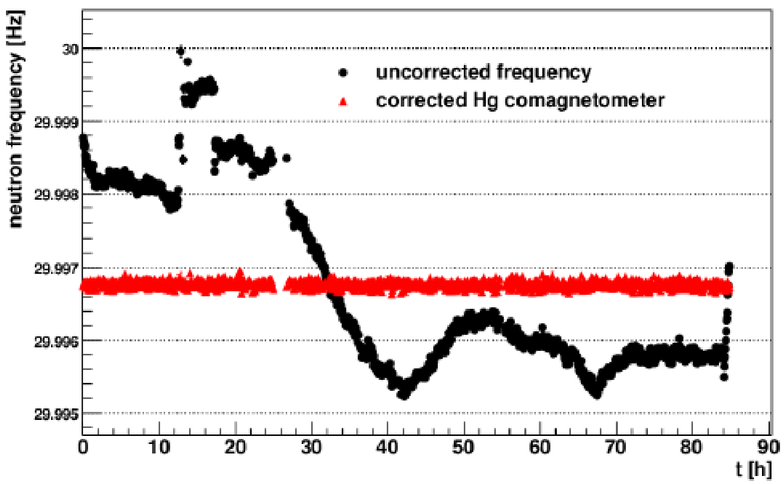

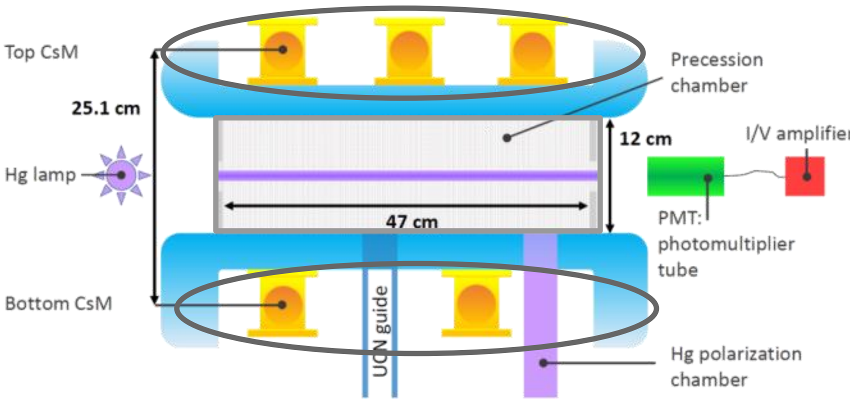

$$R = \frac{\langle f_{\mathrm{UCN}}\rangle}{\langle f_{\mathrm{Hg}}\rangle} = \frac{\gamma_{\mathrm{n}}}{\gamma_{\mathrm{Hg}}}\left(1 \mp \frac{\partial B}{\partial z}\frac{\Delta h}{|B_0|} + \frac{\langle B^2{}_{\perp}\rangle}{|B_0|^2} \mp \delta_{\mathrm{Earth}} + \delta_{\mathrm{Hg-lights}} \ldots\right)$$

Magnetic moments

$$\frac{\gamma_n}{2\pi} = 29.164705(55)\ \mathrm{MHz/T}$$

[1.89 ppm]

γ_{Hg}

$$\gamma_n/\gamma_{Hg} = 3.8424574(30)$$

[0.78 ppm]

γ_n

$$\frac{\gamma_{Hg}}{2\pi} = 7.5901152(62)\ \mathrm{MHz/T}$$

[0.82 ppm]

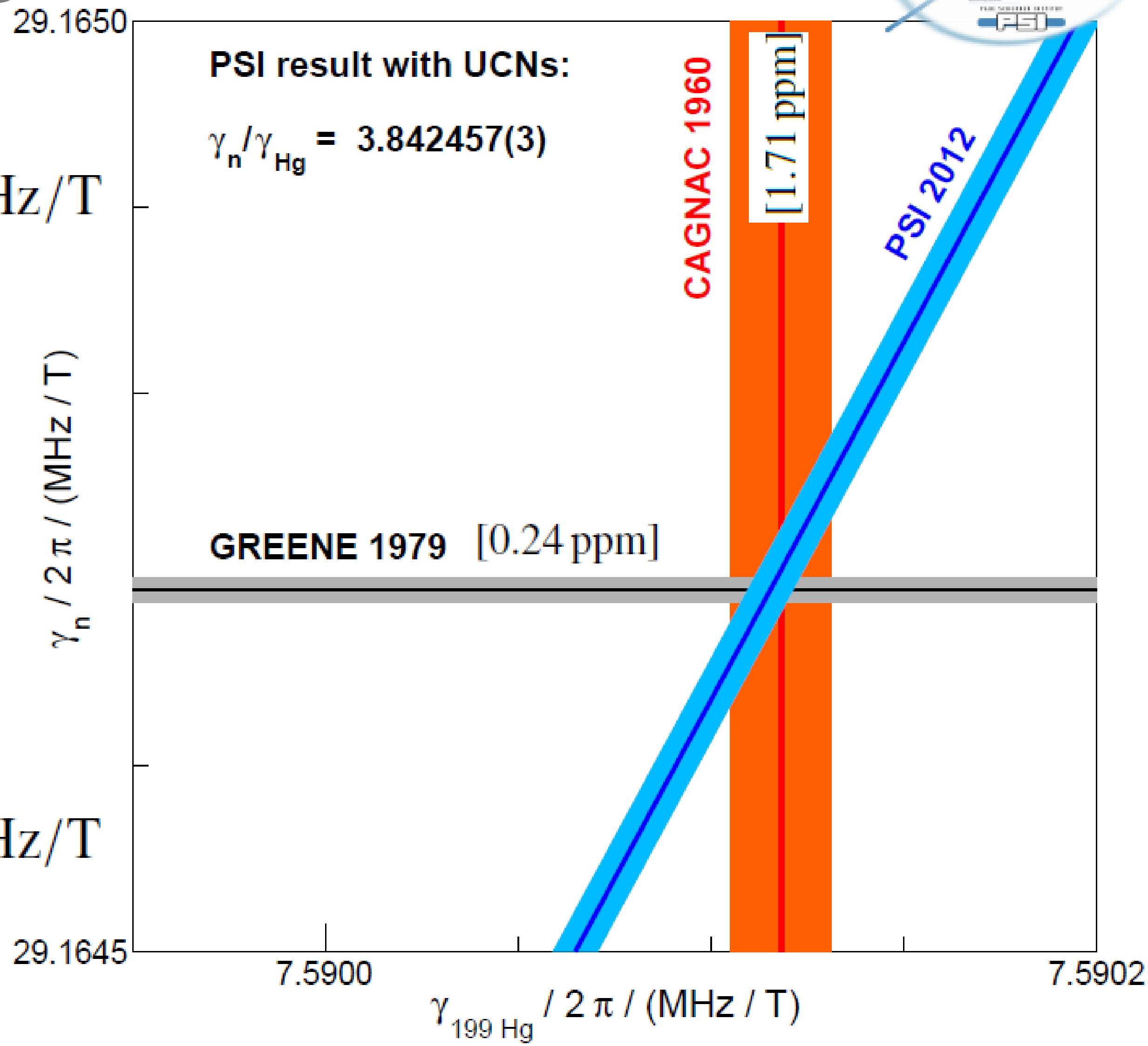

S. Afach et al., PLB 739 (2014) 128

Spin-dependent exotic interactions

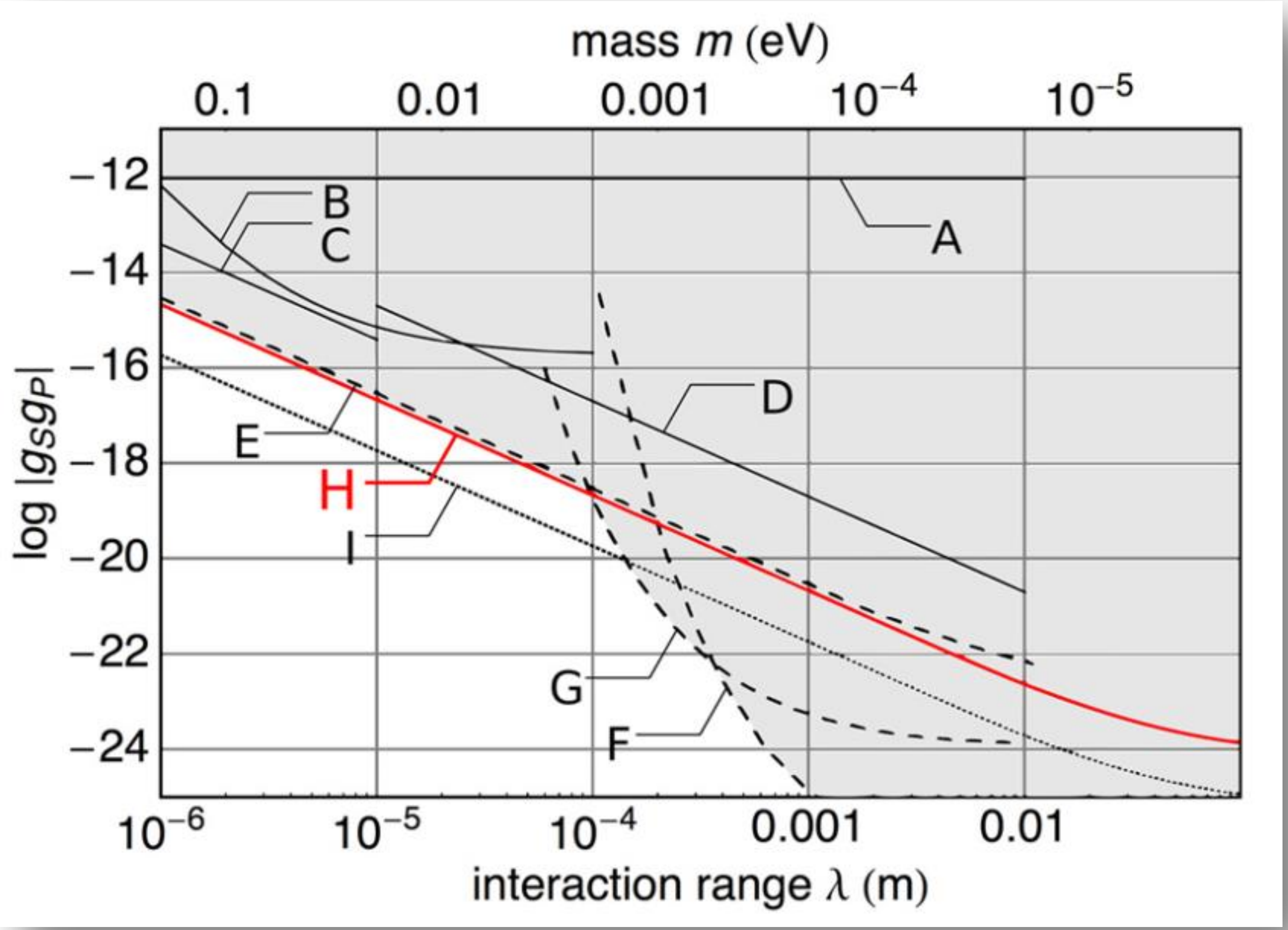

S. Afach et al., PLB 745 (2015) 58

To be updated soon

UCN spin-echo spectroscopy

A spin-echo recovers energy dependent dephasing for $T = 2t_1$ in a magnetic field with vertical gradient.

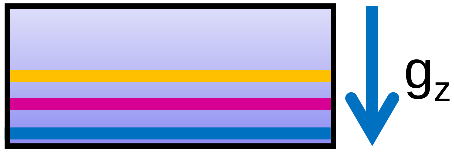

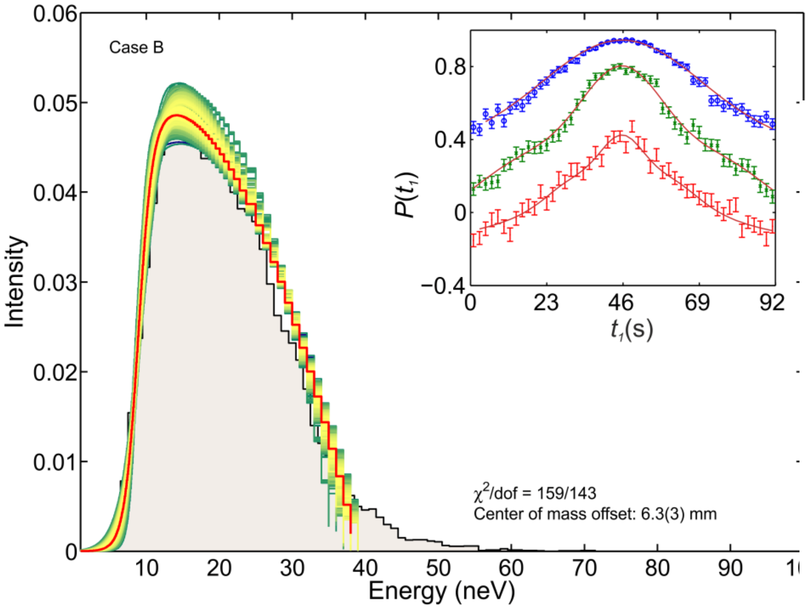

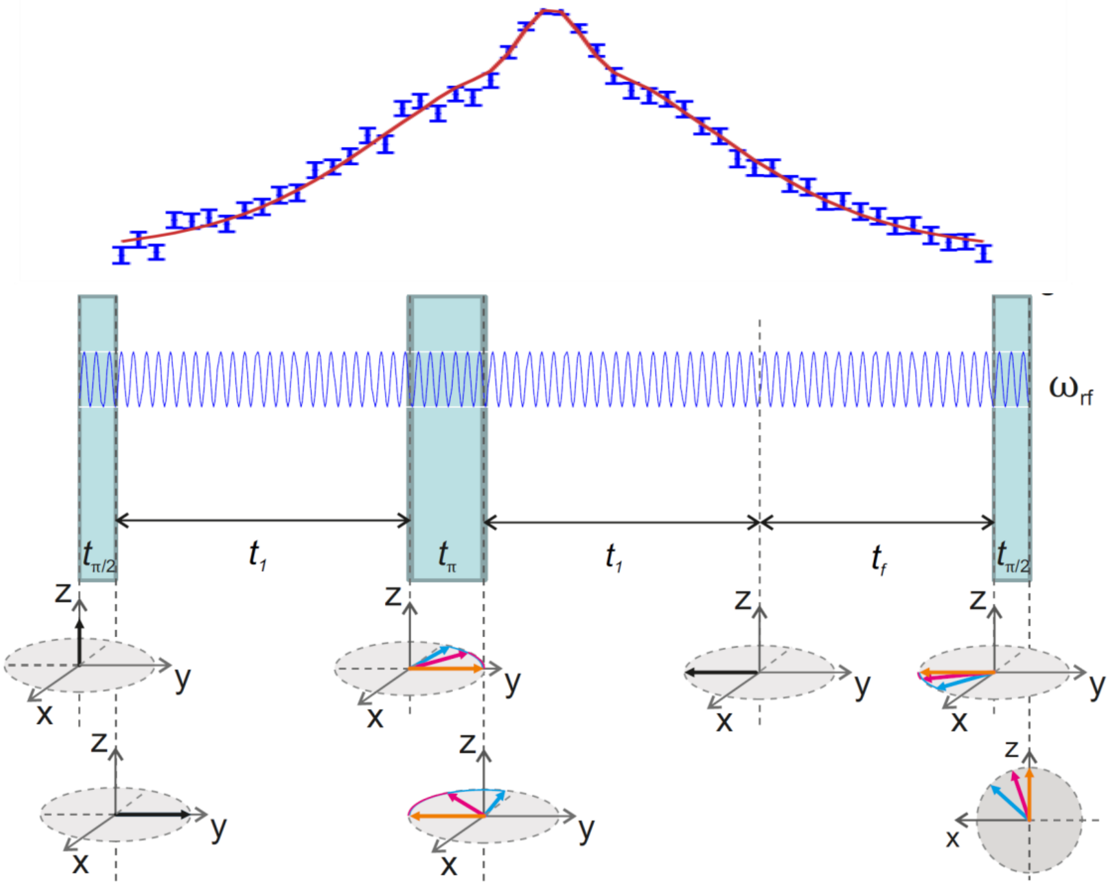

S. Afach et al., PRL114(2015)162502

Earlier results using nEDM

- Searches for nn' oscillations
  - G. Ban *et al.*, PRL99 (2007) 161603
  - I. Altarev *et al*., PRD80 (2009) 03200;
  - to be updated soon …

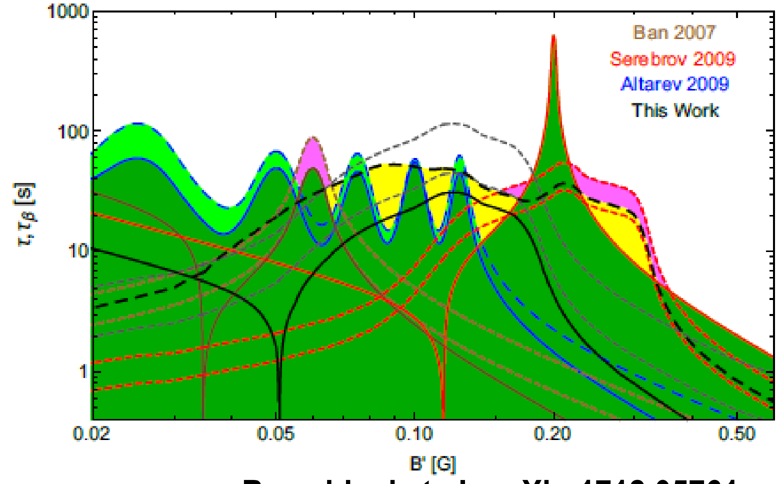

Berezhiani et al., arXiv:1712.05761

- Searches for Lorentz violation
  - I. Altarev *et al.*,PRL 103 (2009) 081602
  - I. Altarev et al., EPL 92 (2010) 51001
  - to be updated soon …

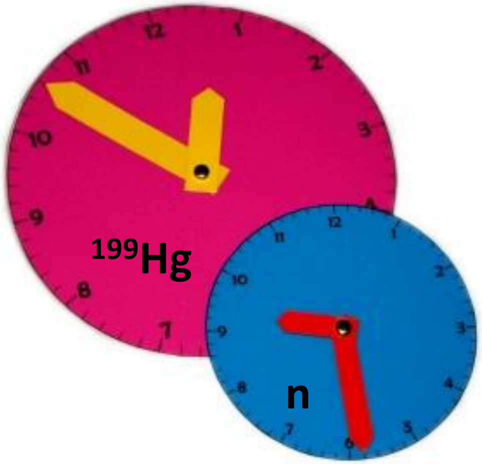

The neutron EDM itself …

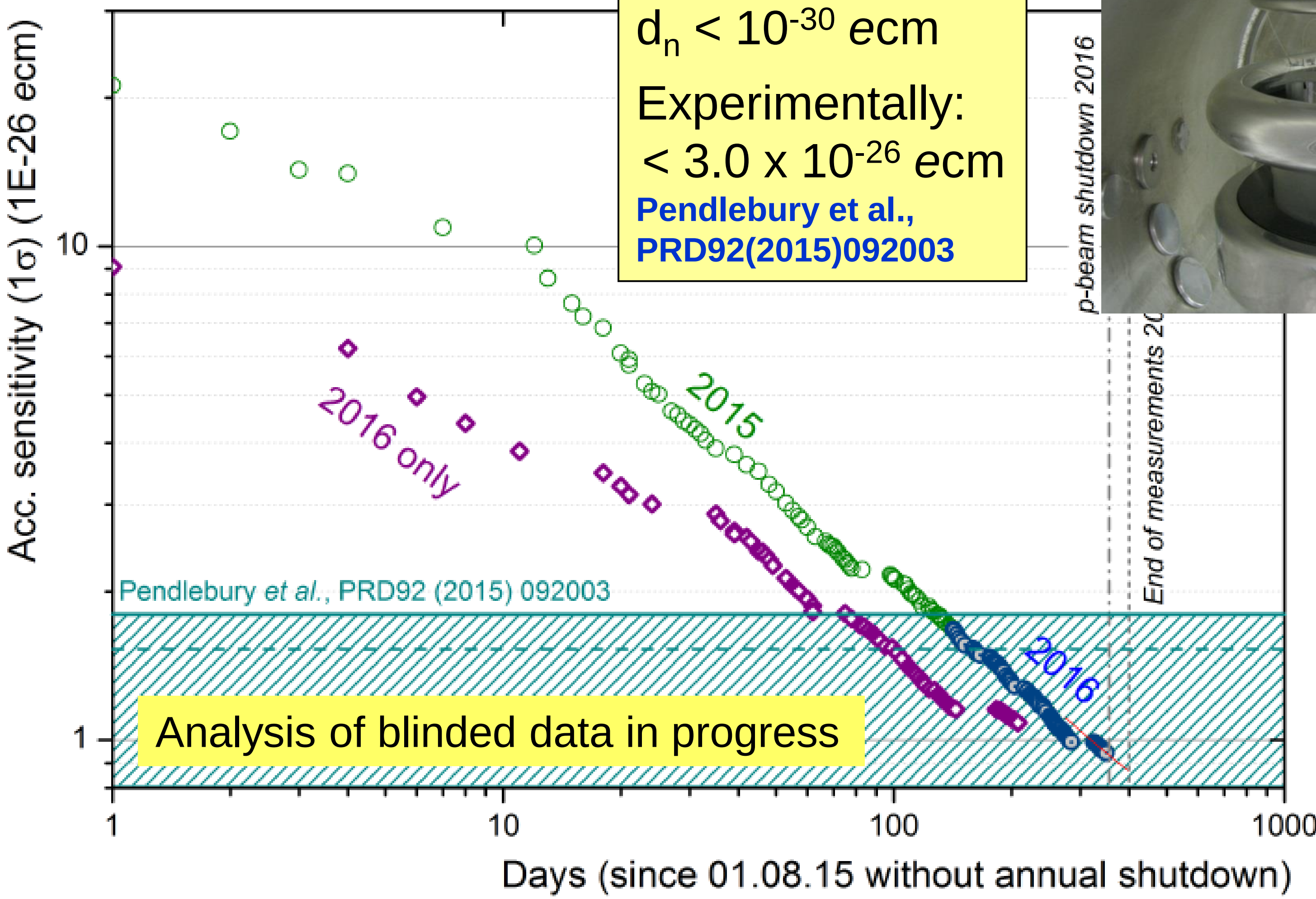

Expect from SM:
$d_n < 10^{-30}$ *e*cm

Experimentally:
$< 3.0 \times 10^{-26}$ *e*cm
Pendlebury et al., PRD92(2015)092003

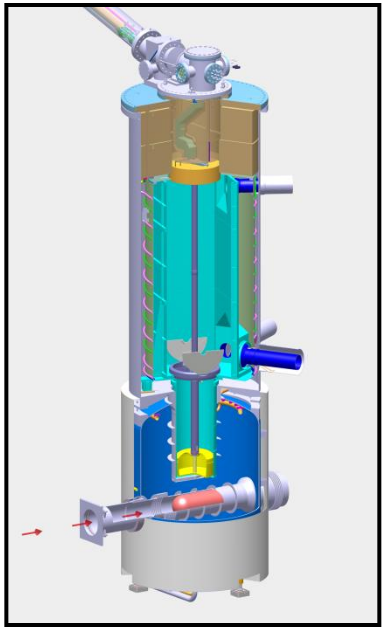

What is the nature of Dark Matter?

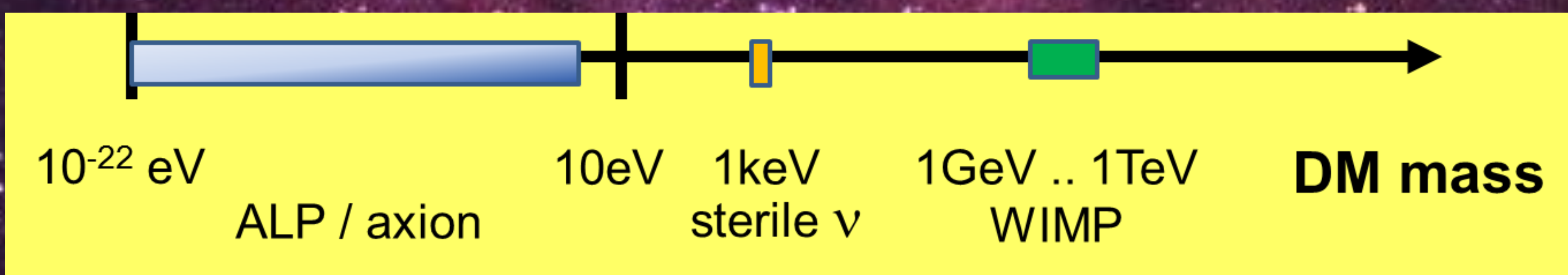

Search for nEDM oscillations with time

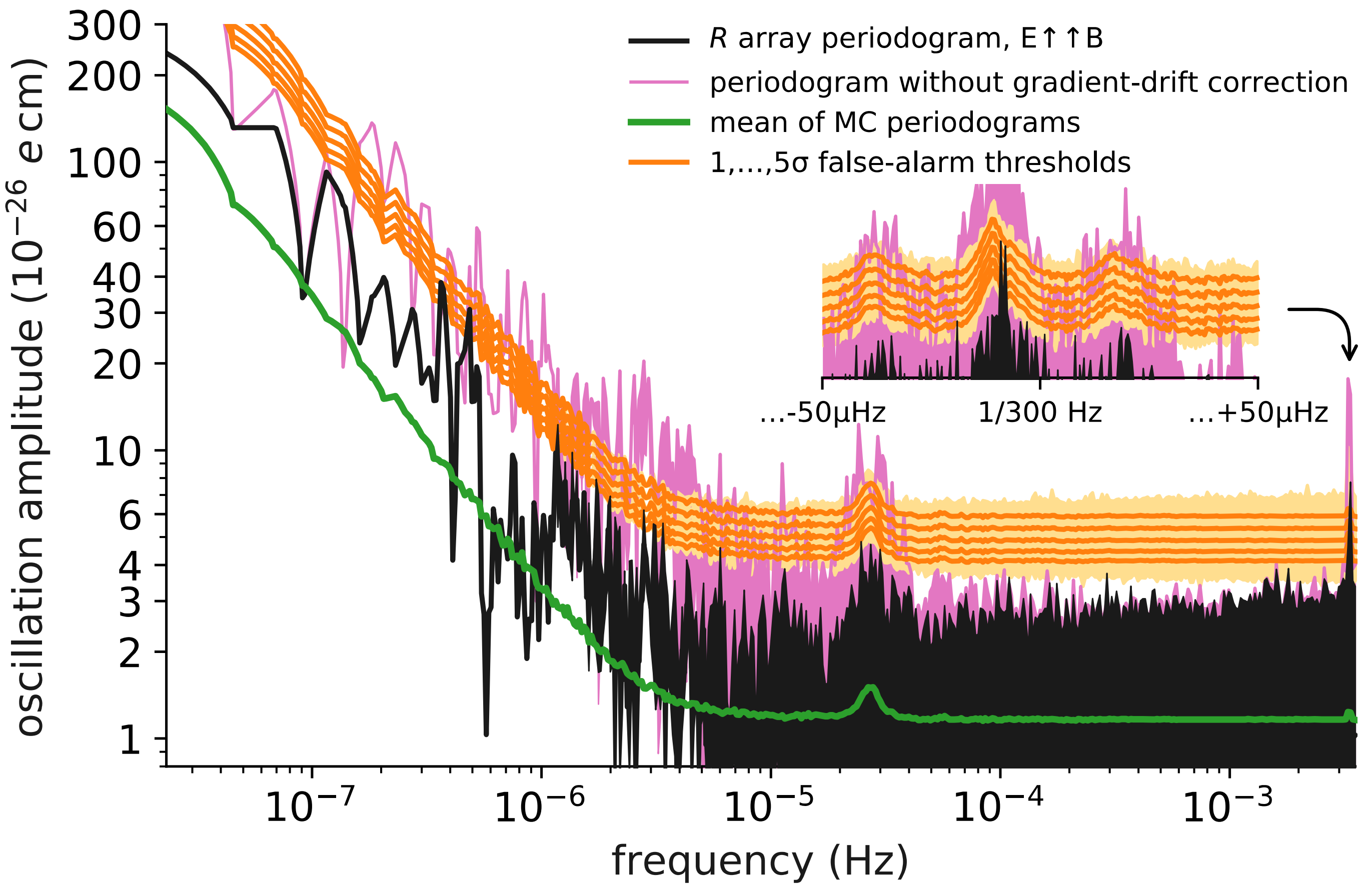

$$d_n(t) = 5.9 \times 10^{-22}\, C_G \left(\frac{10^{-22}\,\mathrm{eV}}{m_a}\right) \left(\frac{10^{16}\,\mathrm{GeV}}{f_a}\right) \cos(m_a t)\ e \cdot \mathrm{cm}$$

Search for nEDM oscillations with time

PHYS. REV. X **7**, 041034 (2017)

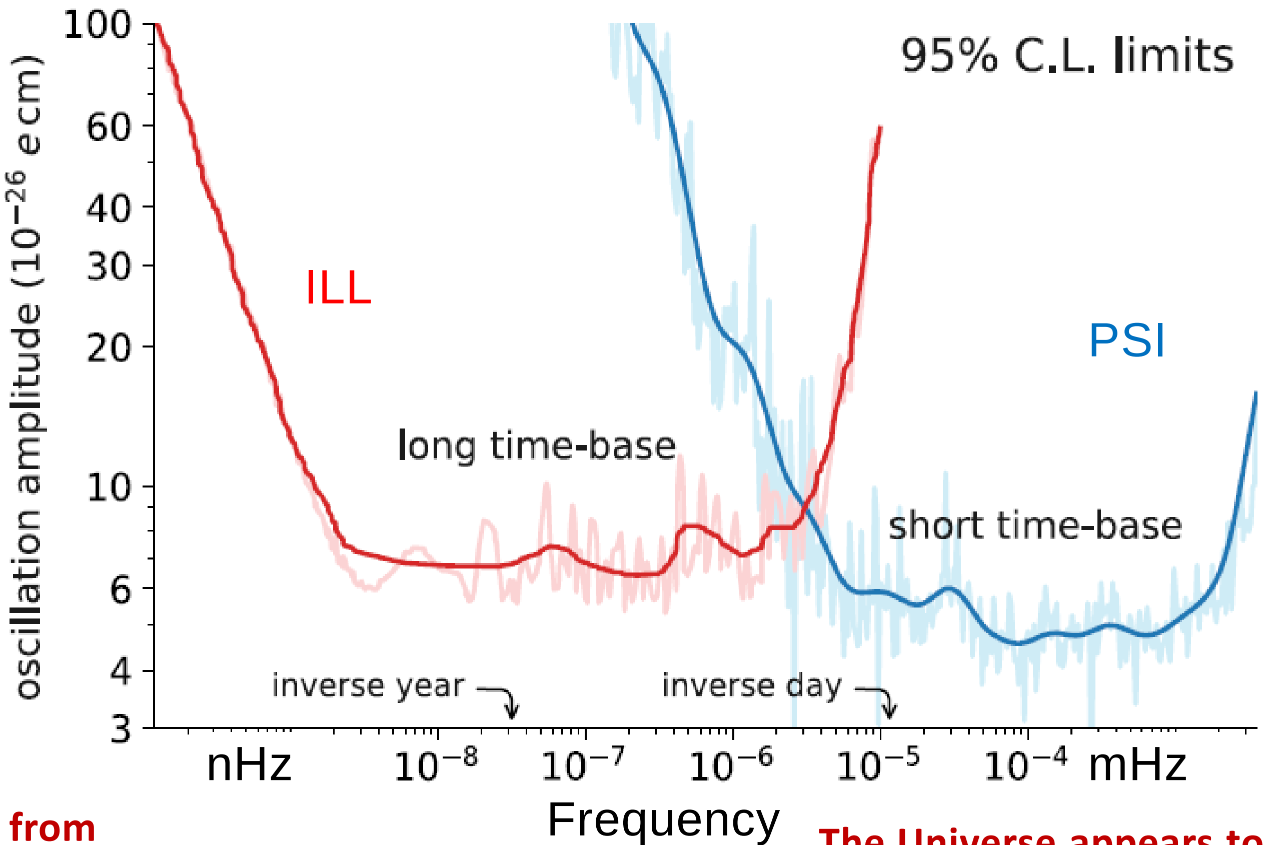

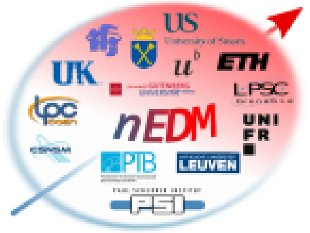

PhD theses
N. Ayres, Sussex
M. Rawlik, ETHZ

nEDM data from
ILL (1998-2002) and PSI (2015-16) has been analyzed for time variations of the nEDM. None have been found, setting the most stringent oscillating EDM limits so far.

The Universe appears to roughly contain
5% ordinary matter (H, He, stars, us, …), 27% **Dark Matter** and 68% Dark Energy. The nature of the Dark components is yet unknown.

nEDM search for ultra-light axion dark matter

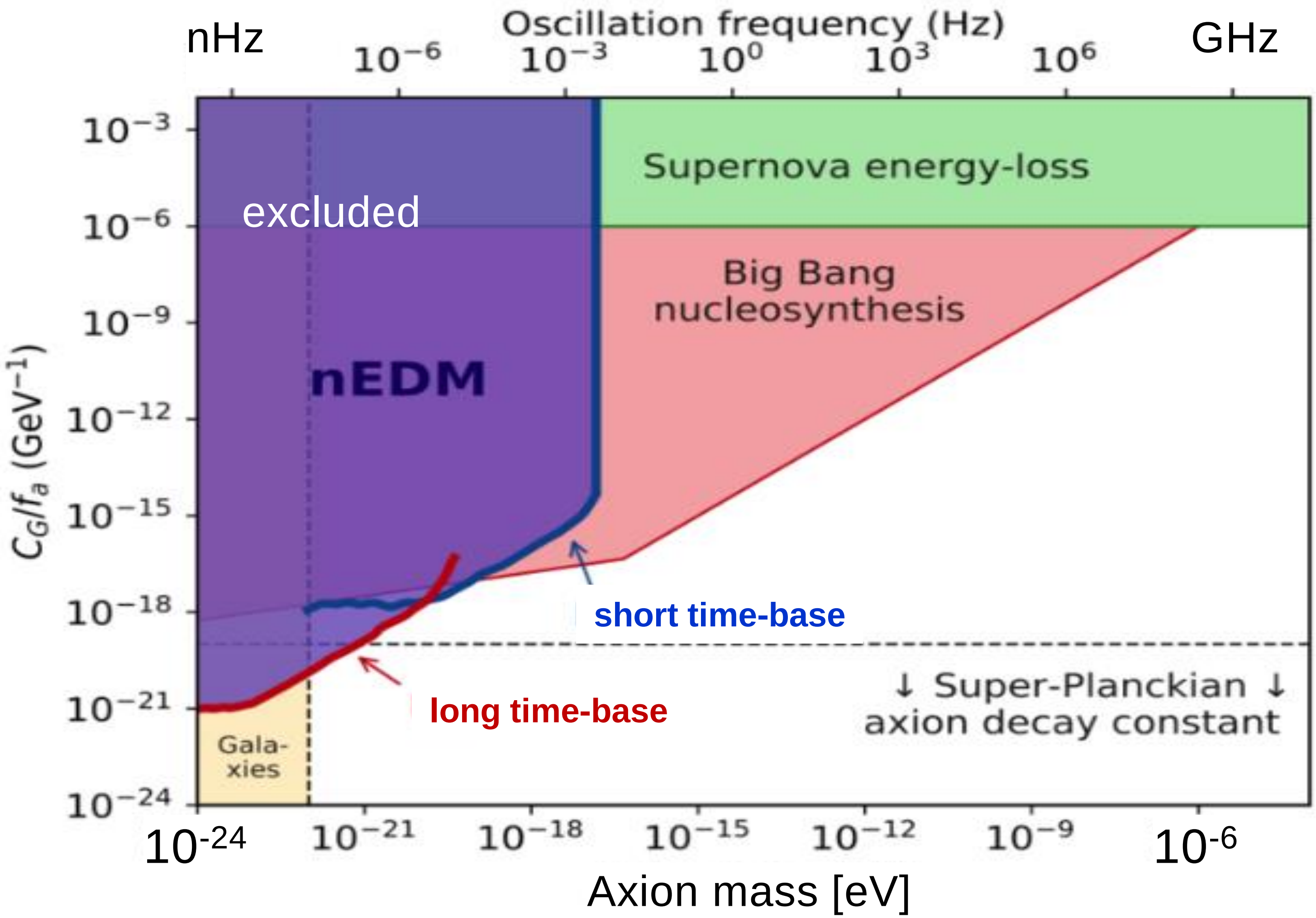

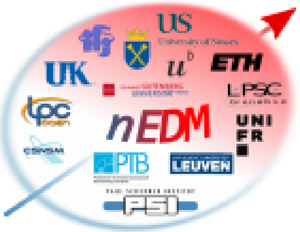

Teamed up with theorists Flambaum, Stadnik, Fairbairn, Marsh

Oscillating nEDM data could come from the interaction of **ultralight axions** which could be the **Dark Matter in the Universe**.

nEDM places the first laboratory limits. on **axion – gluon** couplings

Abel et al., PRX7(2017)041034

Extrapolation to storage ring EDM

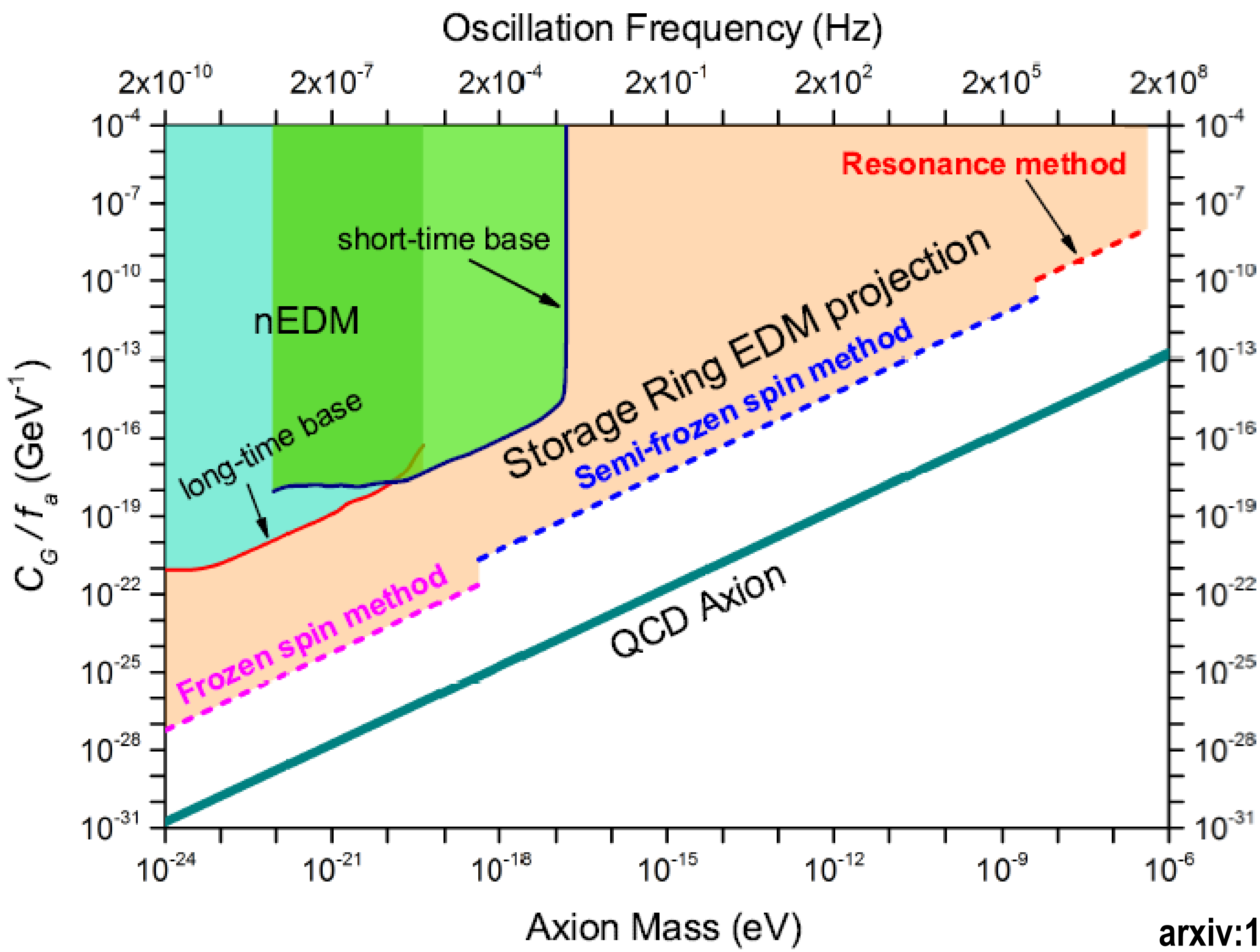

arxiv:1710.05271

2018: n2EDM at PSI

2018: n2EDM at PSI

2018: n2EDM at PSI

Sept

n2EDM baseline:

$\sigma(d_n)$~1E-27*e*cm in 500 days

Commissioning 2020

2018: n2EDM at PSI

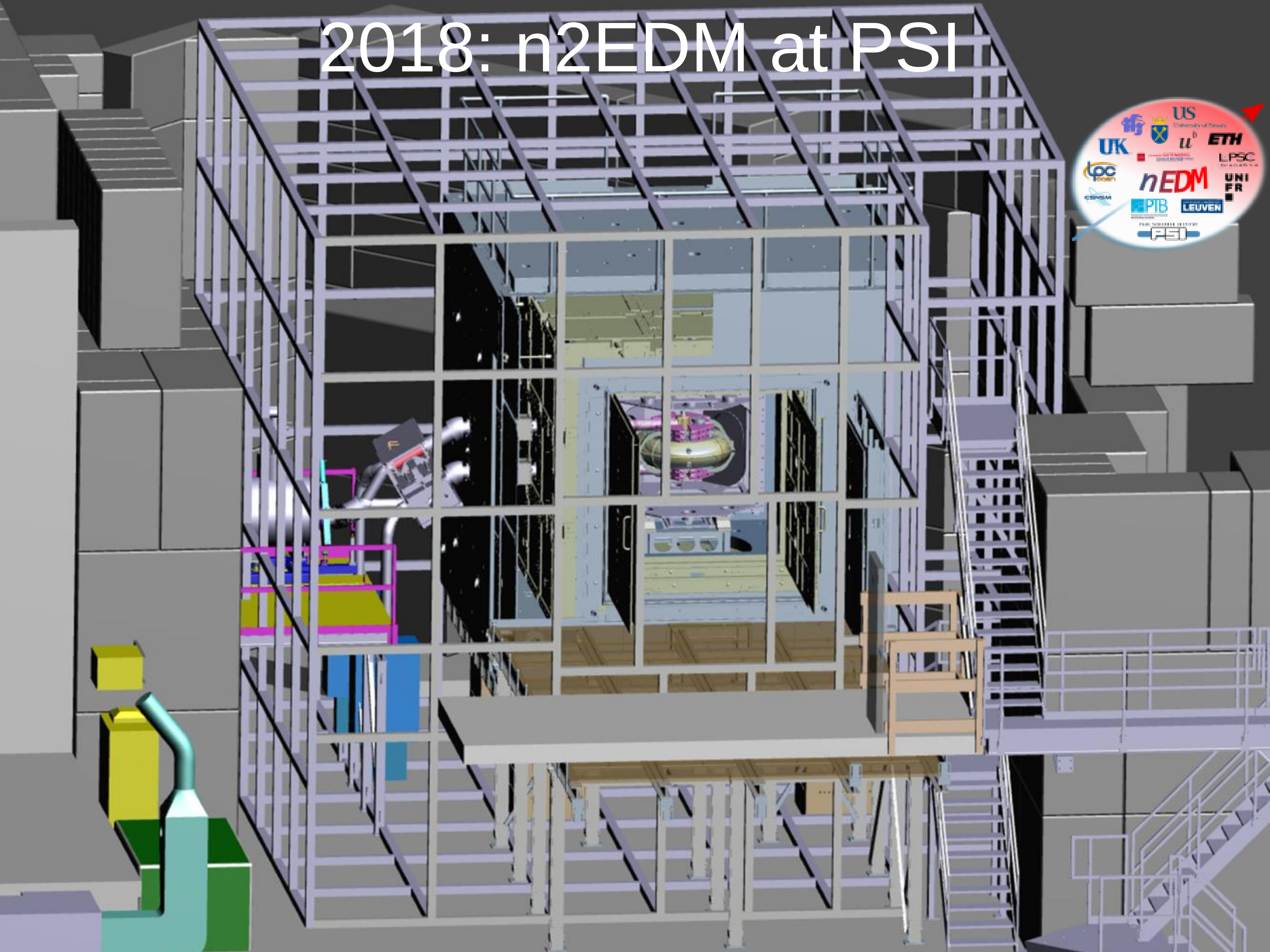

Storage ring EDM

Muon spin precession in *B* and *E* field

Muon spin precession in the presence of *B* and *E* field,
perpendicular to each other and to the muon momentum:

$$\vec{\omega} = -\frac{e}{m}\left\{ \underbrace{a\vec{B} + \left(\frac{1}{1-\gamma^2} - a\right)\frac{\vec{\beta}\times\vec{E}}{c}}_{\vec{\omega}_a} + \underbrace{\frac{\eta}{2}\left(\frac{\vec{E}}{c} + \vec{\beta}\times\vec{B}\right)}_{\vec{\omega}_e} \right\}$$

Example:
B-field pointing down,
E-field radially outward:

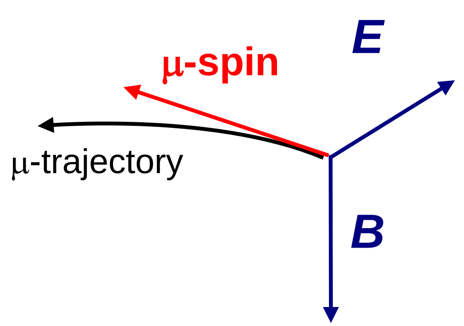

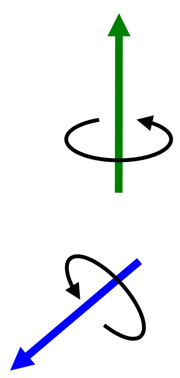

$\vec{\omega}_a$: spin precession in orbital plane
("*g*–2" precession)

$\vec{\omega}_e$: spin precession out of orbital plane

$\vec{\omega} = \vec{\omega}_a + \vec{\omega}_e$ tilts the precession plane out of the orbital plane

Muon spin precession in *B* and *E* field

$$\vec{\omega} = -\frac{e}{m}\left\{\underbrace{a\vec{B} + \cancel{\left(\frac{1}{1-\gamma^2} - a\right)\frac{\vec{\beta}\times\vec{E}}{c}}}_{\vec{\omega}_a} + \underbrace{\frac{\eta}{2}\left(\frac{\vec{E}}{c} + \vec{\beta}\times\vec{B}\right)}_{\vec{\omega}_e}\right\}$$

Strategy for *g*–2 measurement at storage rings:

- run at **"magic γ"**, γ = 29.3 (p_μ= 3.1 GeV)

  ⇒ no effect from electric fields, can use **electric focusing**
  (need for uniform *B* field precludes magnetic focusing)

- assume η small for measurement of a

  ⇒ direct access to a if *B* is known

$$\vec{\omega} = -\frac{e}{m}a\vec{B}$$

- look for small vertical oscillation to put a limit on η.
  - All recent limits have been obtained in this way (CERN, Brookhaven)
  - Plagued by systematics: *g*–2 precession interferes strongly!

Muon spin precession in *B* and *E* field

$$\vec{\omega} = -\frac{e}{m}\left\{\underbrace{\xcancel{a\vec{B} + \left(\frac{1}{1-\gamma^2} - a\right)\frac{\vec{\beta}\times\vec{E}}{c}}}_{\vec{\omega}_a} + \underbrace{\frac{\eta}{2}\left(\frac{\vec{E}}{c} + \vec{\beta}\times\vec{B}\right)}_{\vec{\omega}_e}\right\}$$

New method for EDM measurement: the "frozen spin" technique!

- Go to lower momentum, install a **"magic *E* field"** (radially), such that ω_a vanishes completely: $$E \approx aBc\beta\gamma^2$$
- The spin remains parallel to the momentum along the orbit ("frozen spin")
- In the presence of an EDM ($\eta \neq 0$) the spin is slowly rotated out of the orbital plane.
- **Much superior sensitivity** than with parasitic approach!

$$\vec{\omega} = -\frac{e}{m}\frac{\eta}{2}\left(\frac{\vec{E}}{c} + \vec{\beta}\times\vec{B}\right)$$

F. Farley et al.:
New Method of Measuring Electric Dipole Moments in Storage Rings,
Phys. Rev. Lett. 93 (2004) 052001

Proton spin precession in *B* and *E* field

$$\vec{\omega} = -\frac{e}{m}\left\{ \underbrace{\cancel{a\vec{B}} + \cancel{\left(\frac{1}{1-\gamma^2} - a\right)\frac{\vec{\beta}\times\vec{E}}{c}}}_{\vec{\omega}_a} + \underbrace{\frac{\eta}{2}\left(\frac{\vec{E}}{c} + \cancel{\vec{\beta}\times\vec{B}}\right)}_{\vec{\omega}_e} \right\}$$

New method for proton EDM measurement: "frozen spin + electrostatic"

- run at **"magic γ"**, (p_p= 0.7 GeV, E=233 MeV), need no magnetic field

  ⇒ all electric storage ring

- The spin remains parallel to the momentum along the orbit ("frozen spin")
- In the presence of an EDM ($\eta \neq 0$) the spin is slowly rotated out of the orbital plane.
- Many systematic controls, CW/CCW, …

arxiv:1502.04317

Storage ring EDM

- CPEDM collaboration proposing proton EDM in (400m) electrostatic ring at CERN, ultimately to 1E-29ecm (or even beyond)
(see e.g. arxiv:1502.04317)
  - 30m prototype planned

- JEDI in Jülich to demonstrate method in COSY (magnetic ring) for deuteron to about 1E-20ecm
(PR Accel. Beams 20(2017)072801, arxiv:1703.01295)

- Dedicated small muon ring experiment at PSI?
(JPG37(2010)085001)

Possibility for a large Muon EDM?

- In a model independent approach, d_μ uniquely constrains some couplings (M. Pruna arXiv:1710.08311), d_μ is not limited by small d_e but only by the direct experimental limit $d_\mu<1.8\times10^{-19}$ecm (Bennett et al., PRD80(2009)052008)
- If NP in a_μ → d_μ could naturally be of same order, ~10^{-22}ecm (Feng, Matchev, Shadmi, NPB613(2001)366)
- If NP in a_μ and a_e (with the sign of the slight tension in a_e)
  → muon and electron sectors would be decoupled
  → large d_μ possible (Crivellin, Hoferichter, Schmidt-Wellenburg, arXiv:1807.11484)
- Present g-2 experiment will improve sensitivity to d_μ~$10^{-20..21}$ecm
- Dedicated small storage ring could reach d_μ~$10^{-22..23}$ecm at PSI (Adelmann et al., JPG37(2010)085001)

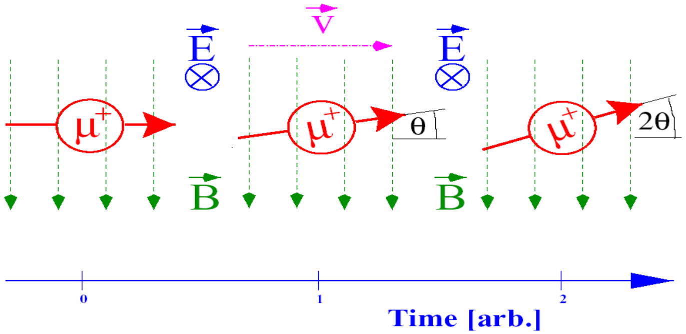

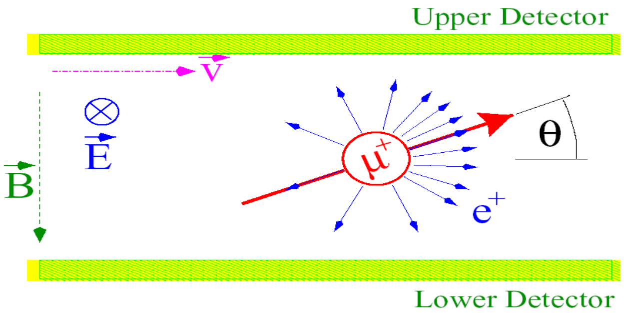

Artist's impression (A. Streun)

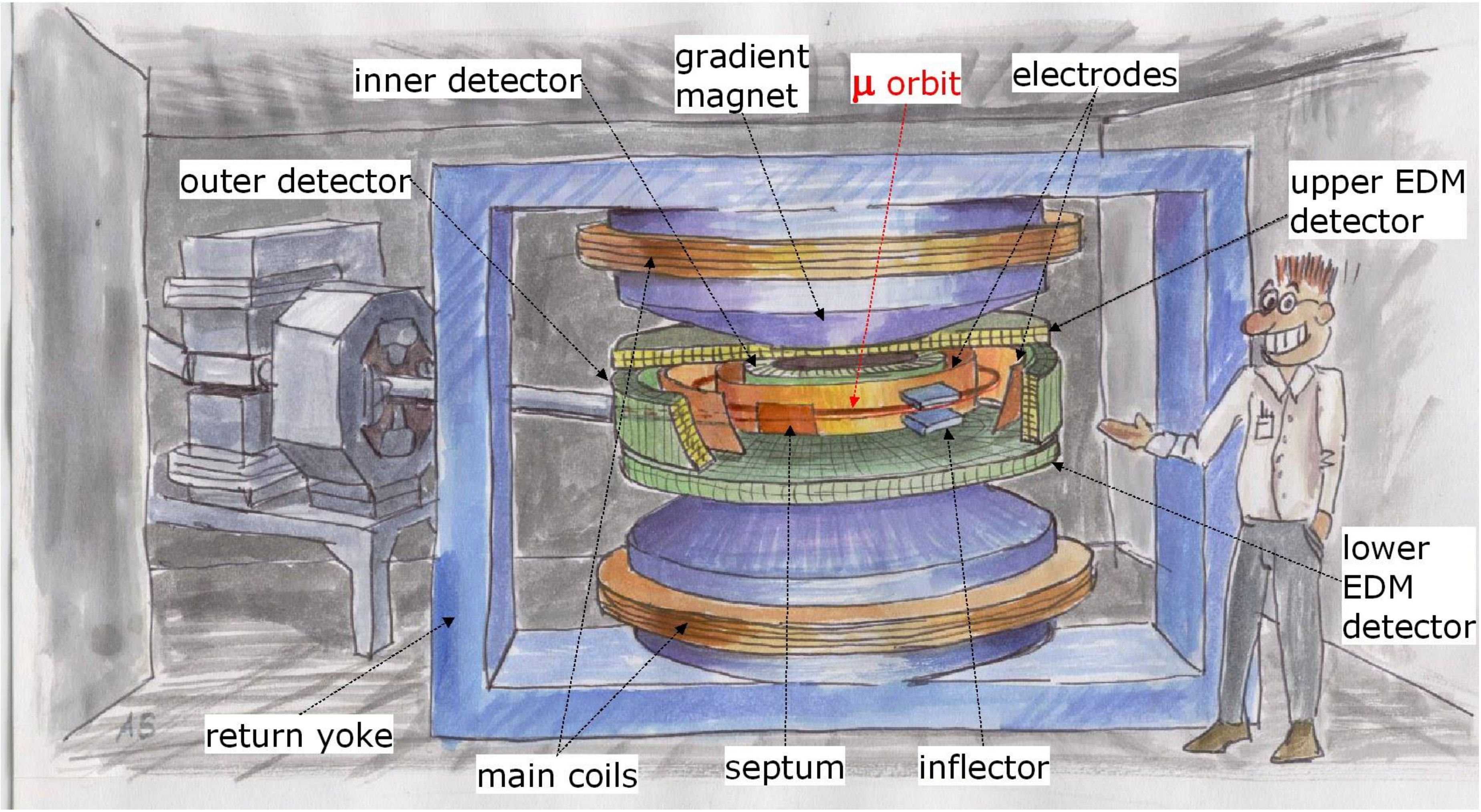

Perhaps we should stop here …

Next future 2020s perspectives

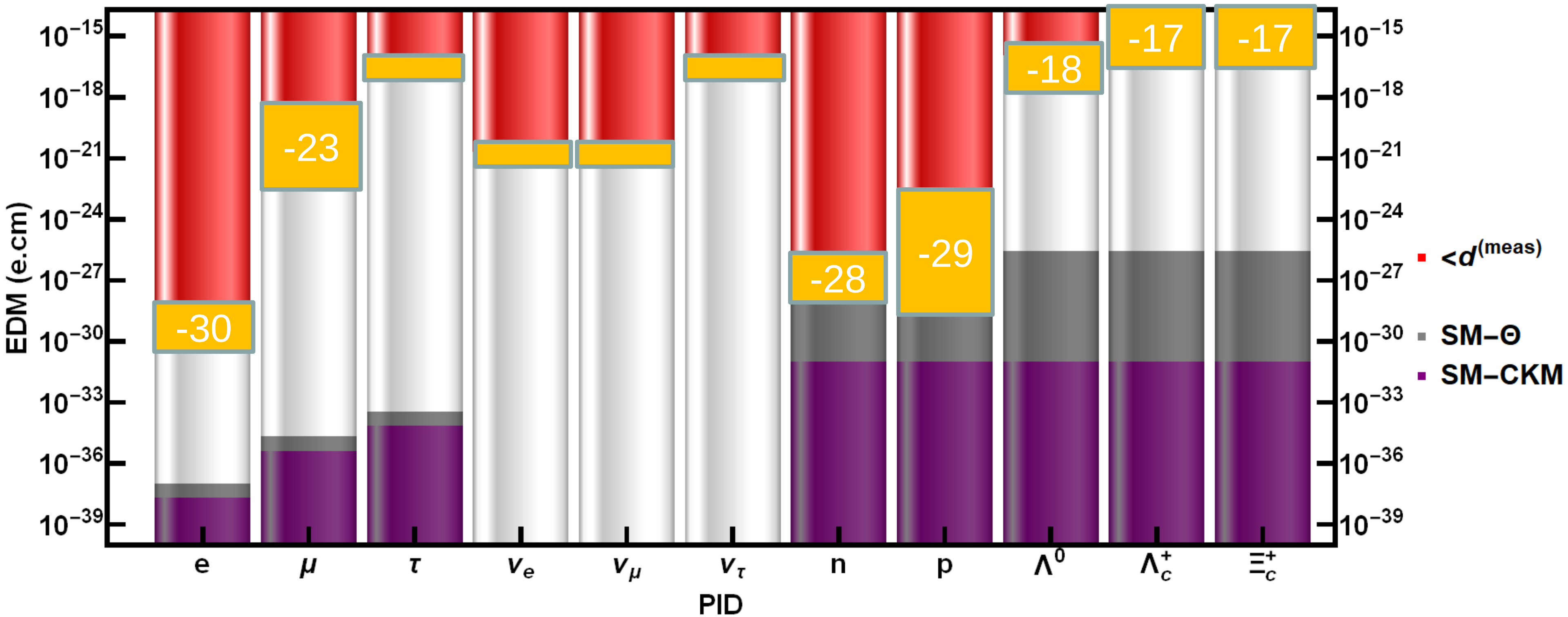

Based on reasonable extrapolation and author claims

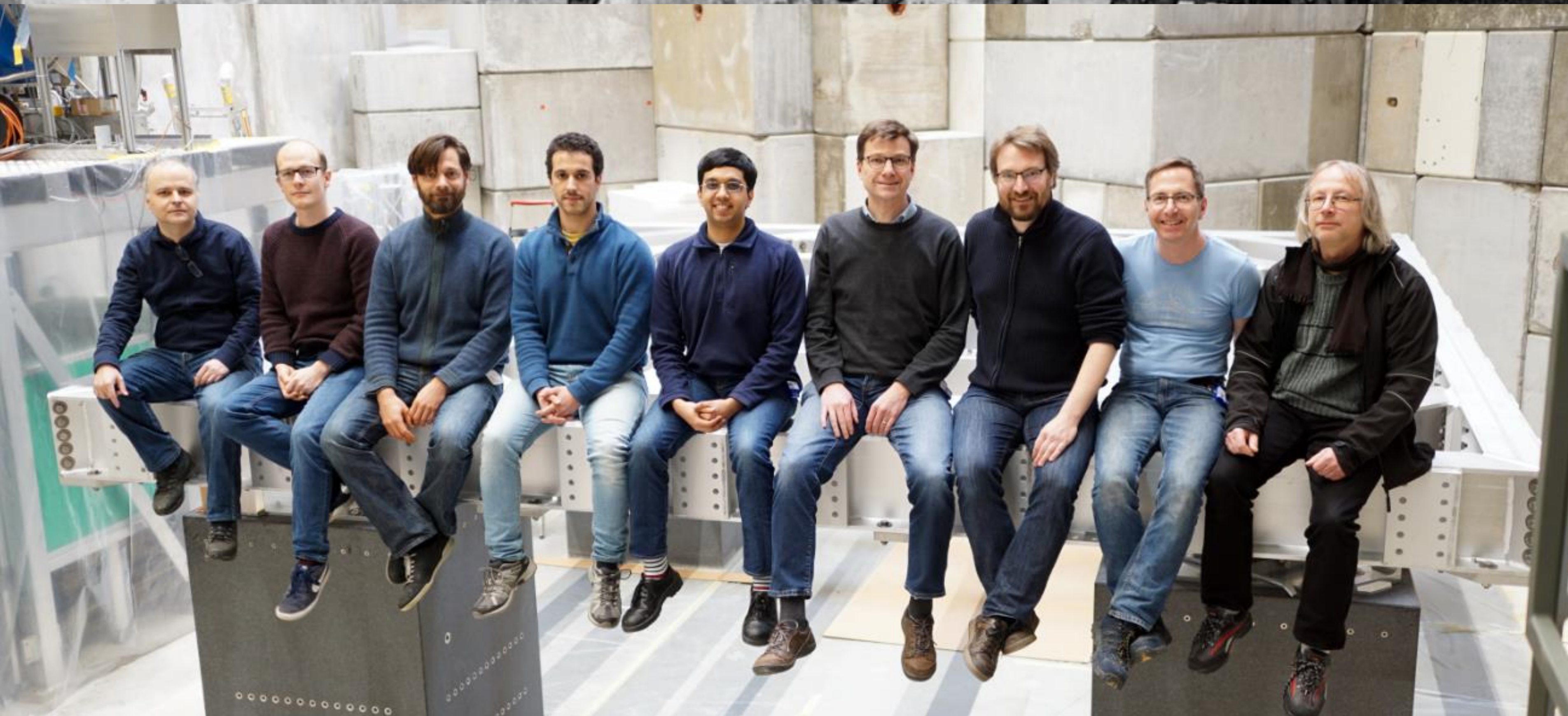


Thank you
arts-wallpapers.com
- Not for Sale

Backup

UCN sources and nEDM experiments

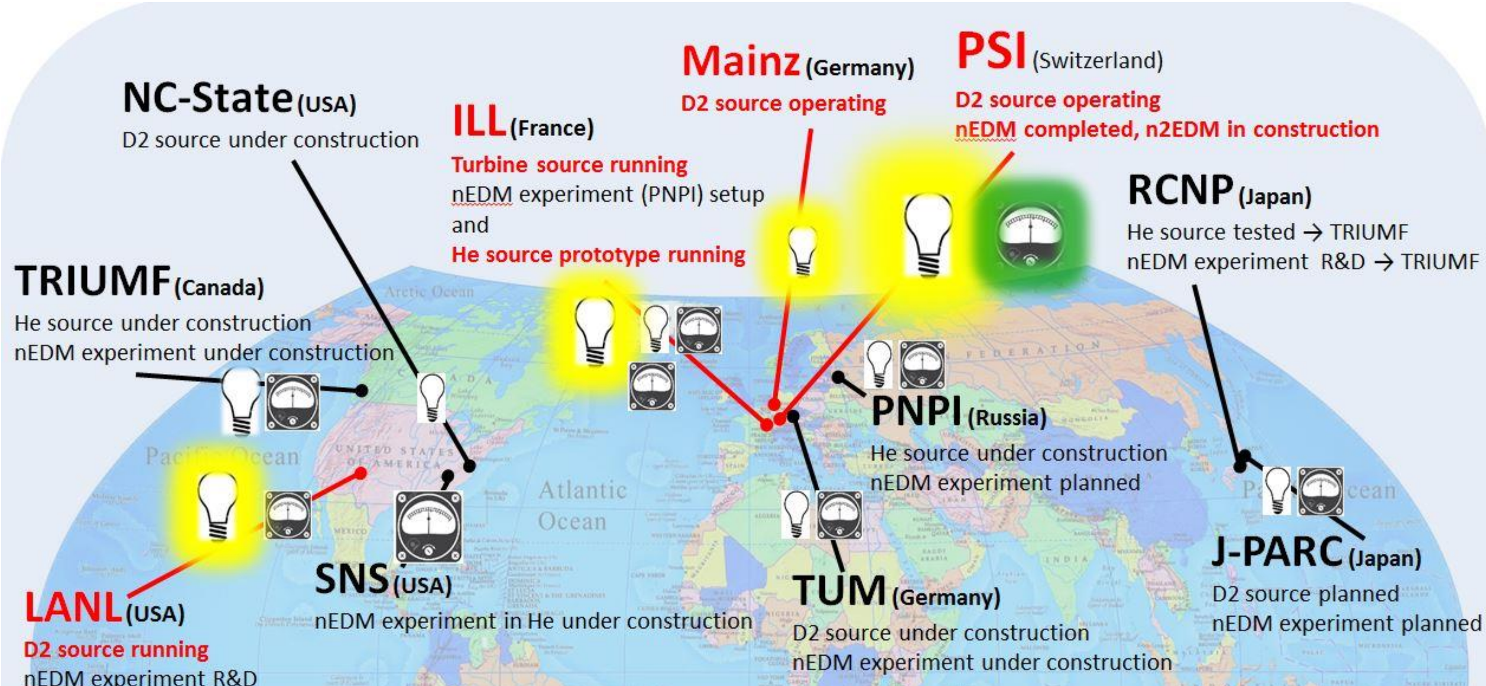

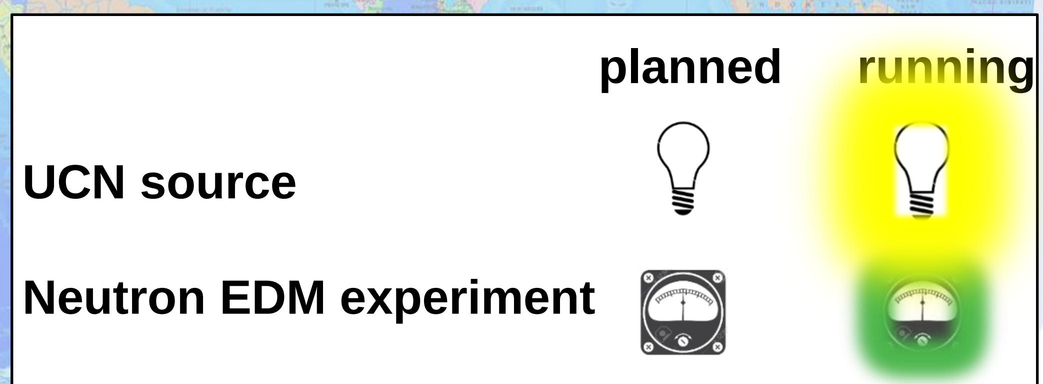

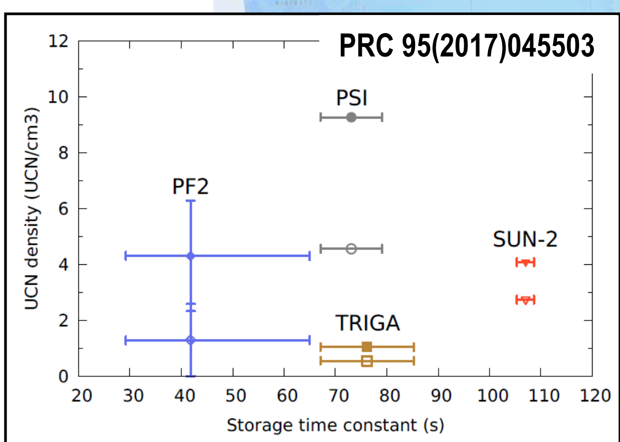

nEDM@PSI

Our collaboration (50 people, 15 institutions, 7 countries) just finished nEDM and starts assembling the n2EDM experiment aiming at an improvement in sensitivity by an order of magnitude.

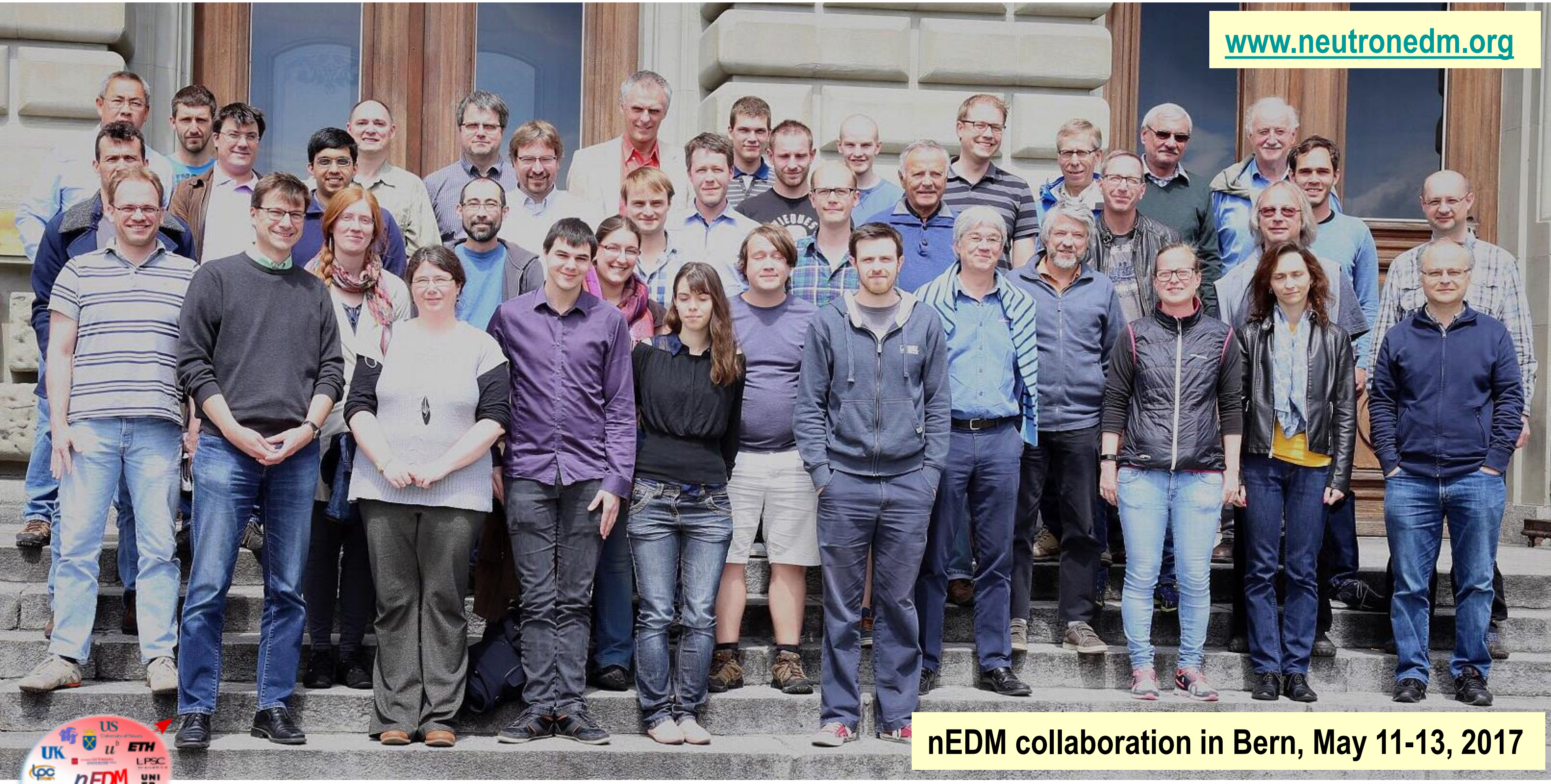

nEDM is presently being taken apart

nEDM is presently being taken apart

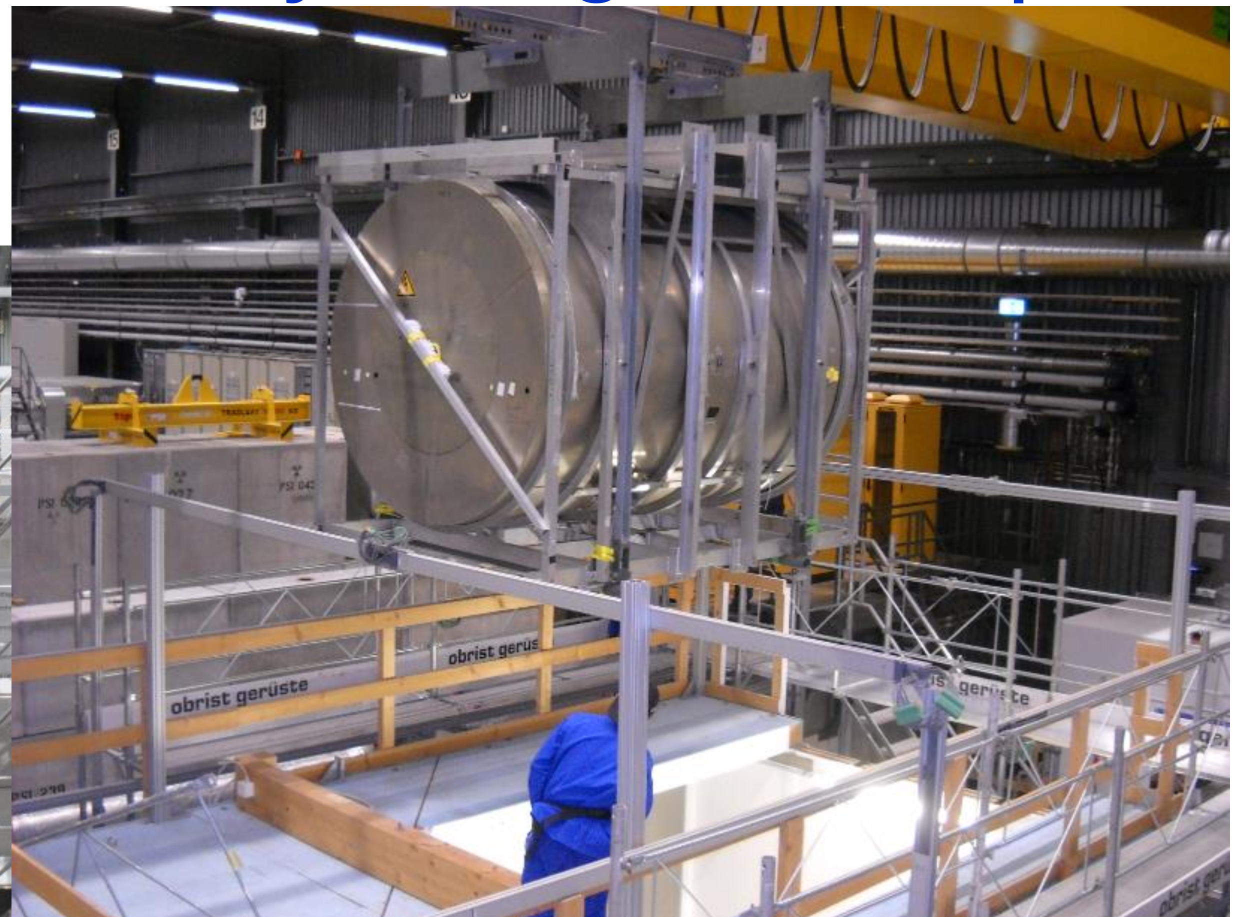

PSI ring cyclotron

- at time of construction a new concept: separated sector ring cyclotron [H.Willax et al.]
- 8 magnets (280t, 1.6-2.1T), 4 accelerating resonators (50MHz), 1 Flattop (150MHz), ∅ 15m
- losses at extraction ≤ 200W
- reducing losses by increasing RF voltage was main upgrade path

[losses ∝ (turn number)^3, W.Joho]

- 590MeV protons at 80%c
- 2.4mA x 590MeV=1.4MW

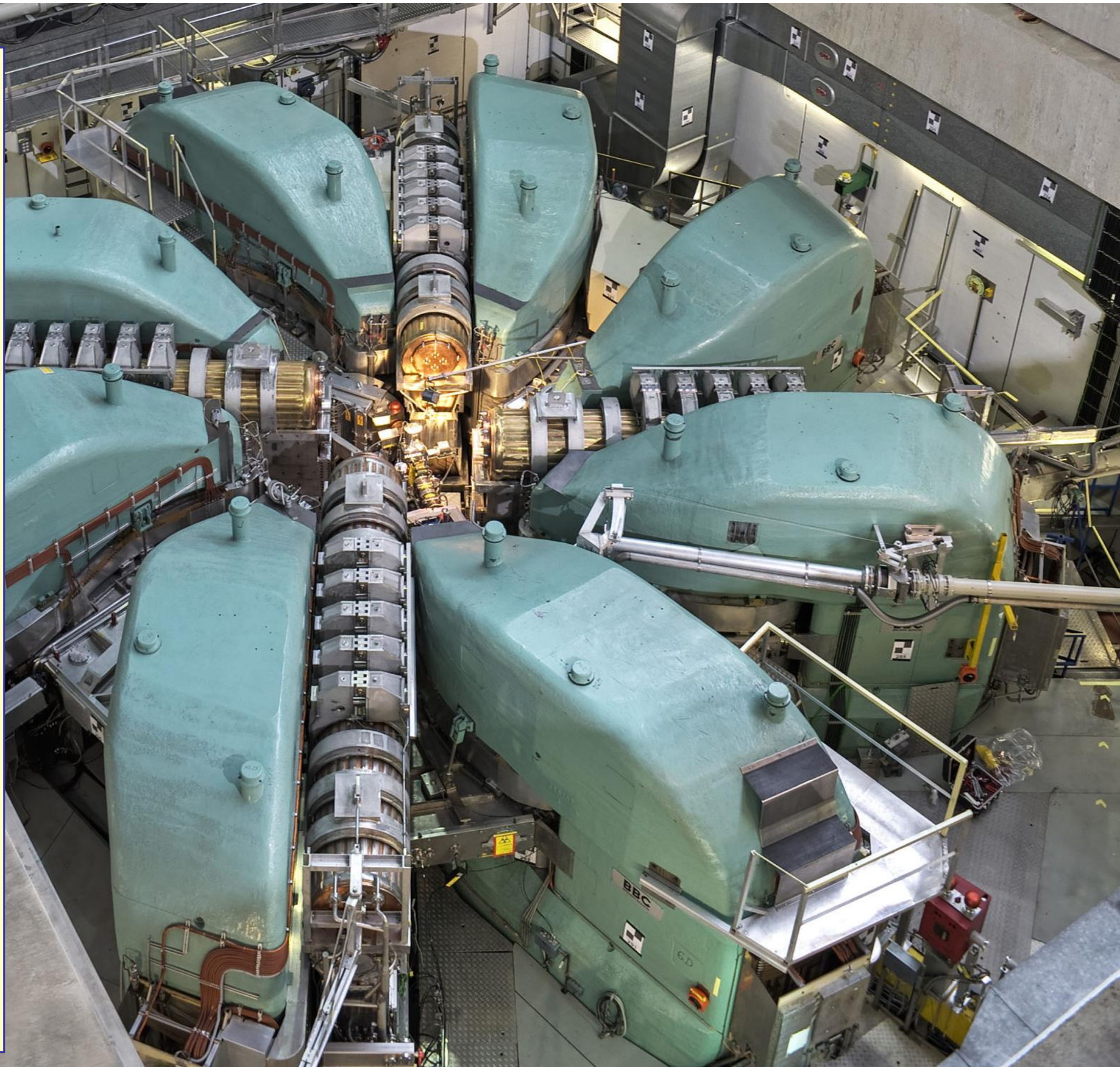

PSI ring cyclotron

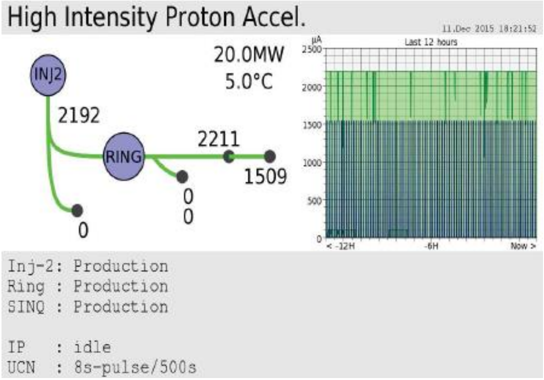

The most powerful
proton beam to targets:
590 MeV x 2.4 mA = 1.4 MW

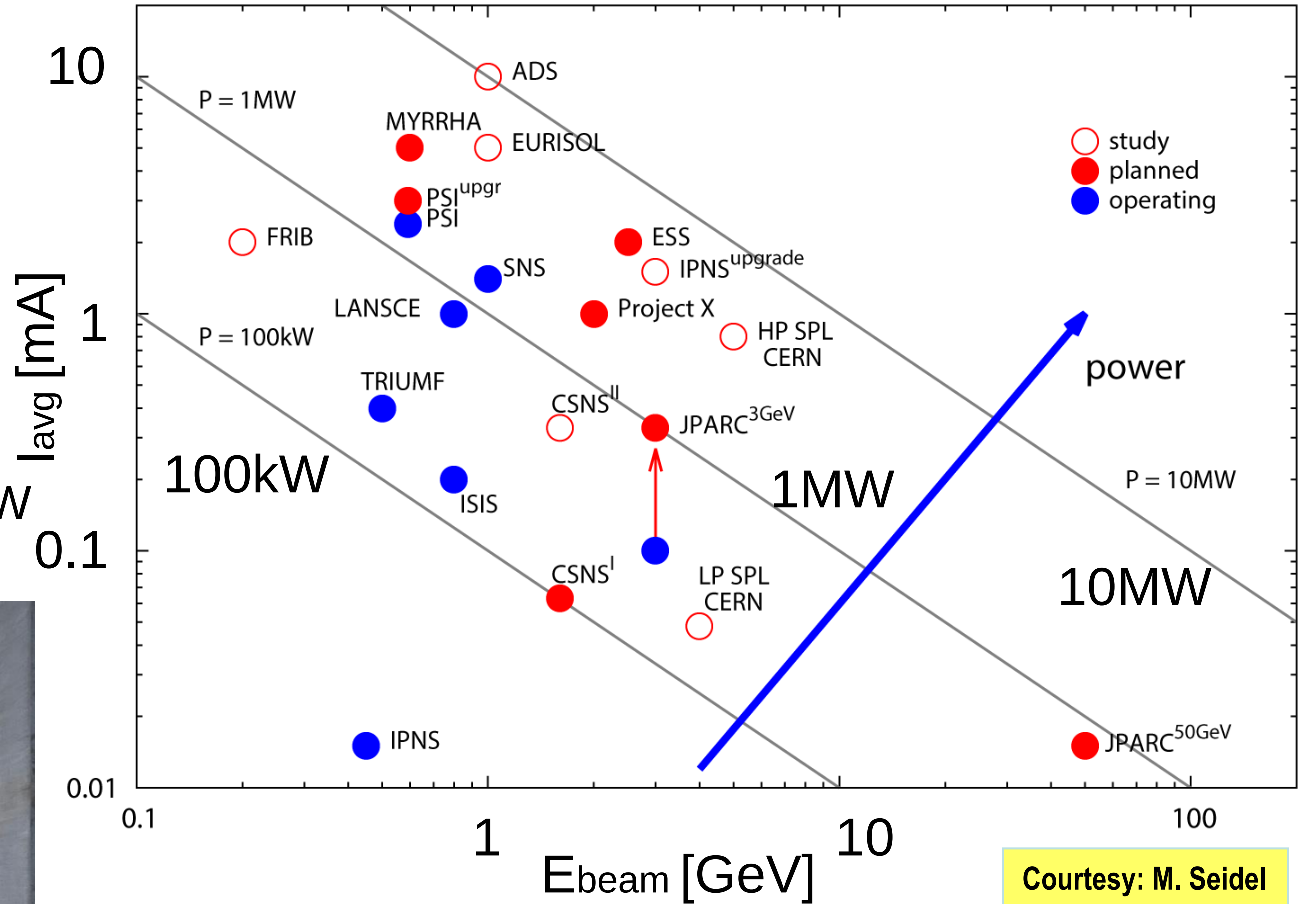

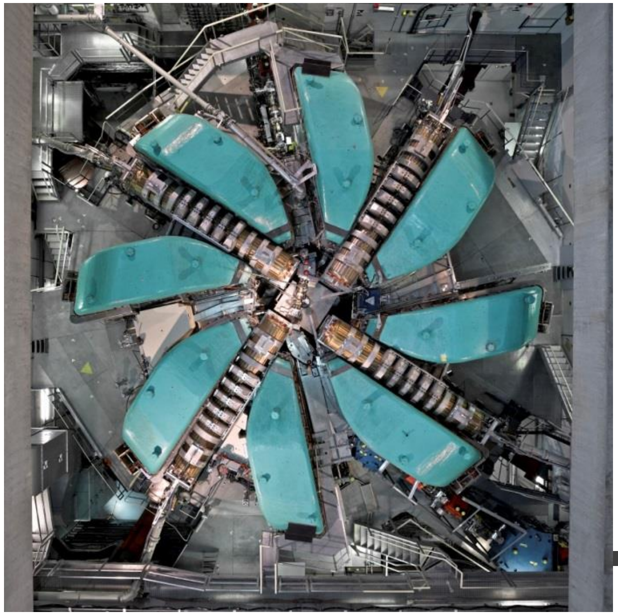

HIPA at PSI is a leading machine at the intensity frontier.
It produces the highest intensities of muons and pions
at low momenta and of ultracold neutrons.